# Digital Image Processing

## Chapter 3: Intensity Transformations and Spatial Filtering

# Background

- Spatial domain process

$$g(x,y) = T[f(x,y)]$$

  - where $f(x,y)$ is the input image, $g(x,y)$ is the processed image, and T is an operator on f, defined over some neighborhood of $(x,y)$

- Neighborhood about a point

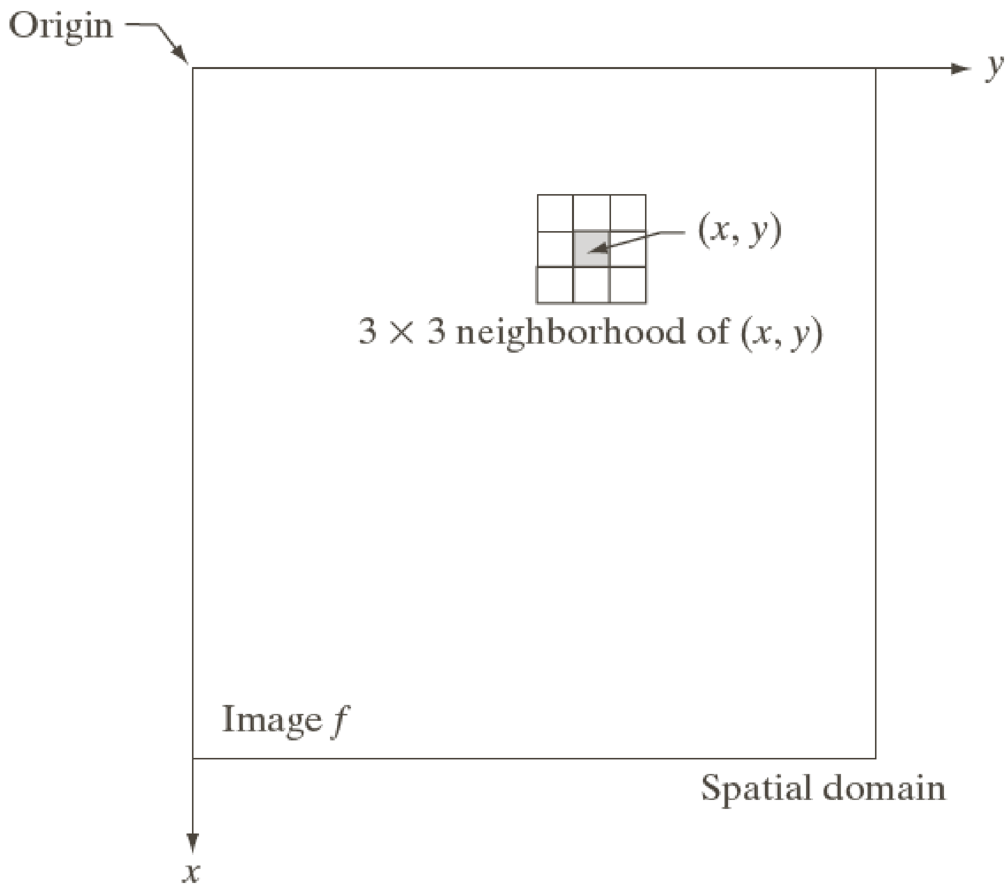


**FIGURE 3.1**
A 3 × 3 neighborhood about a point (x, y) in an image in the spatial domain. The neighborhood is moved from pixel to pixel in the image to generate an output image.

- Gray-level transformation function

$$s = T(r)$$

  - where r is the gray level of $f(x, y)$ and s is the gray level of $g(x, y)$ at any point $(x, y)$

- Contrast enhancement
  - For example, a thresholding function

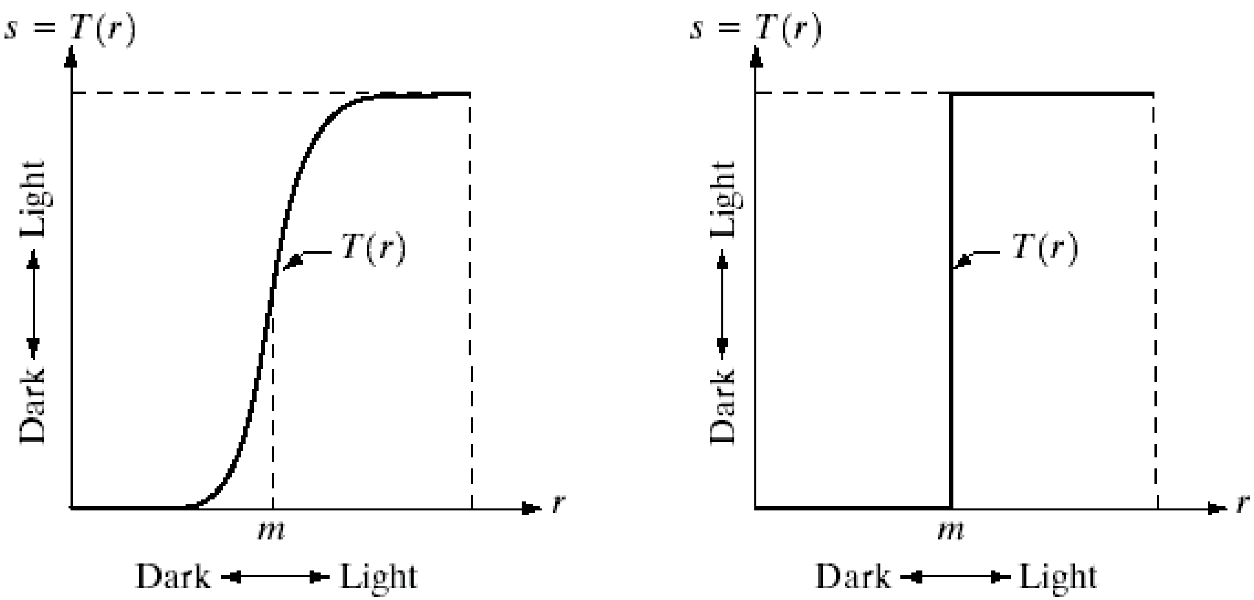


a b

**FIGURE 3.2** Gray-level transformation functions for contrast enhancement.

- Masks (filters, kernels, templates, windows)
  - A small 2-D array in which the values of the mask coefficients determine the nature of the process

# Some Basic Gray Level Transformations

**FIGURE 3.3** Some basic gray-level transformation functions used for image enhancement.

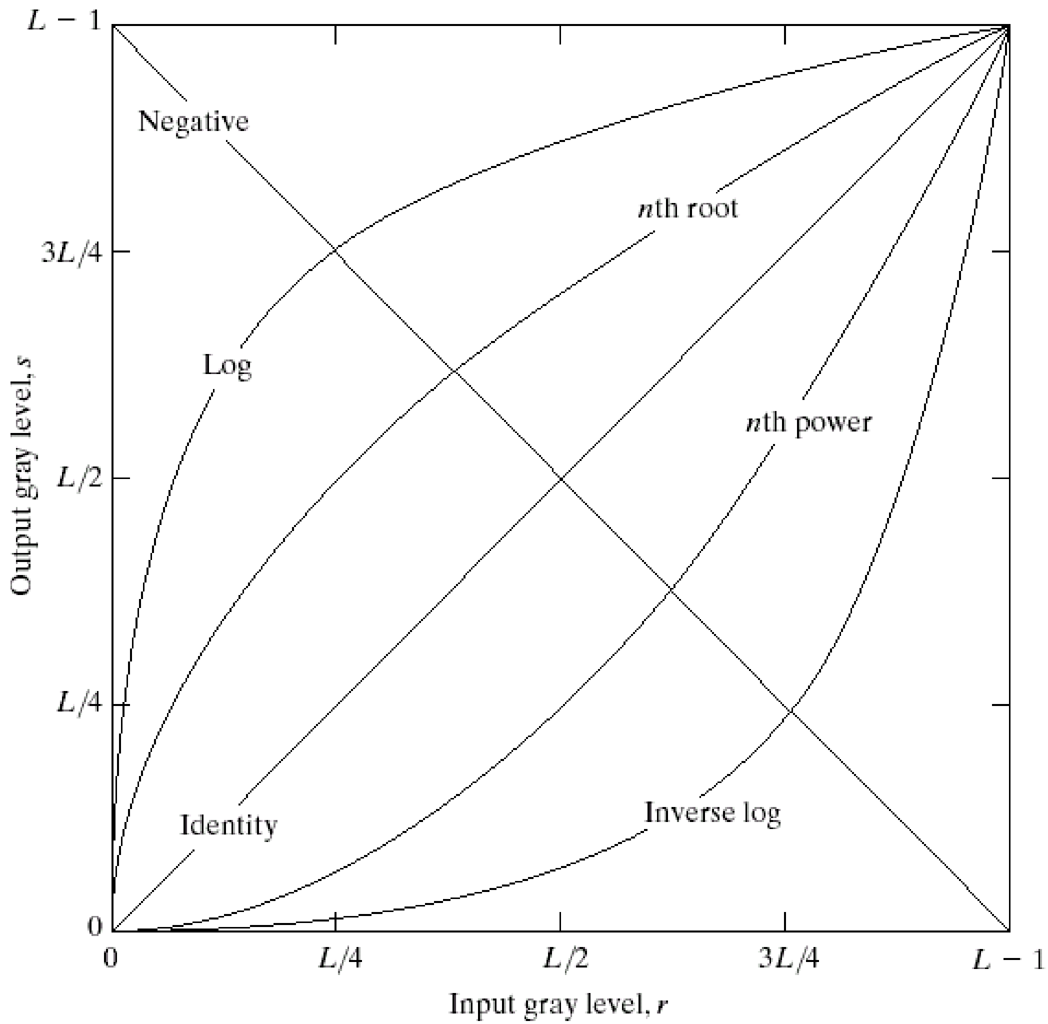

- Image negatives

$$s = L - 1 - r$$

  - Enhance white or gray details

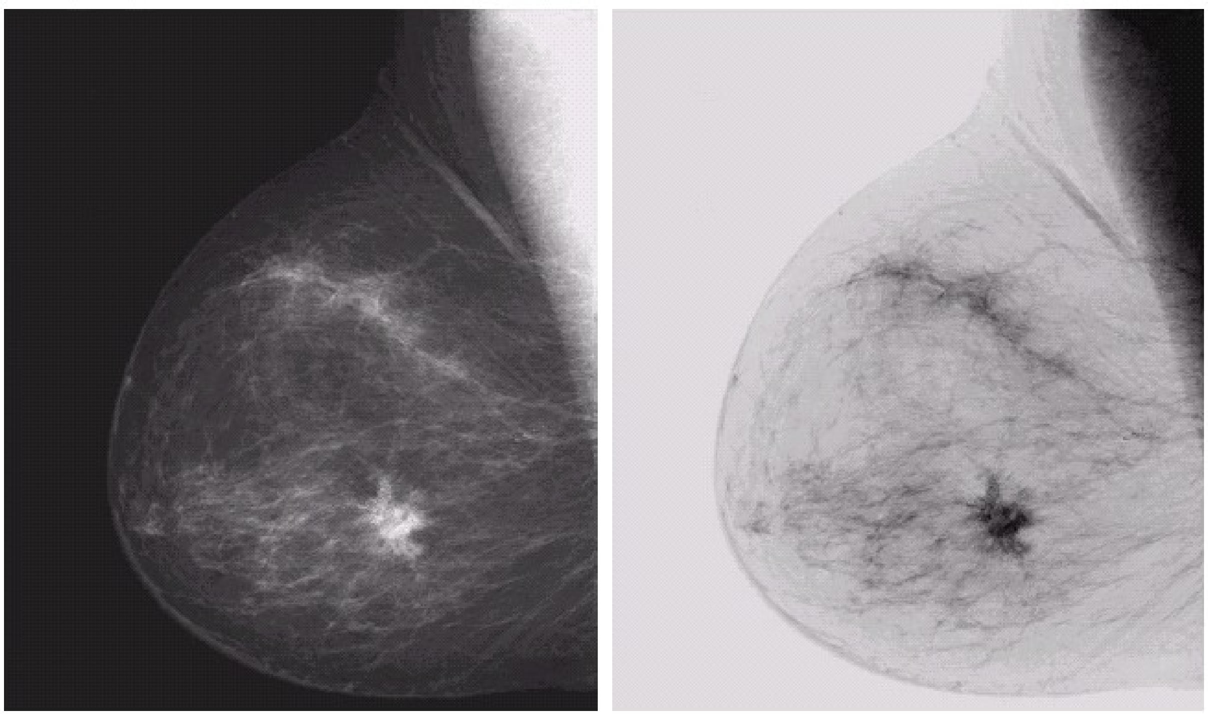

a b

**FIGURE 3.4** (a) Original digital mammogram. (b) Negative image obtained using the negative transformation in Eq. (3.2-1). (Courtesy of G.E. Medical Systems.)

- Log transformations

$$s = c\log(1+r)$$

  - Compress the dynamic range of images with large variations in pixel values

- From the range 0-$1.5 \times 10^6$ to the range 0 to 6.2

a b

**FIGURE 3.5** (a) Fourier spectrum. (b) Result of applying the log transformation given in Eq. (3.2-2) with $c = 1$.

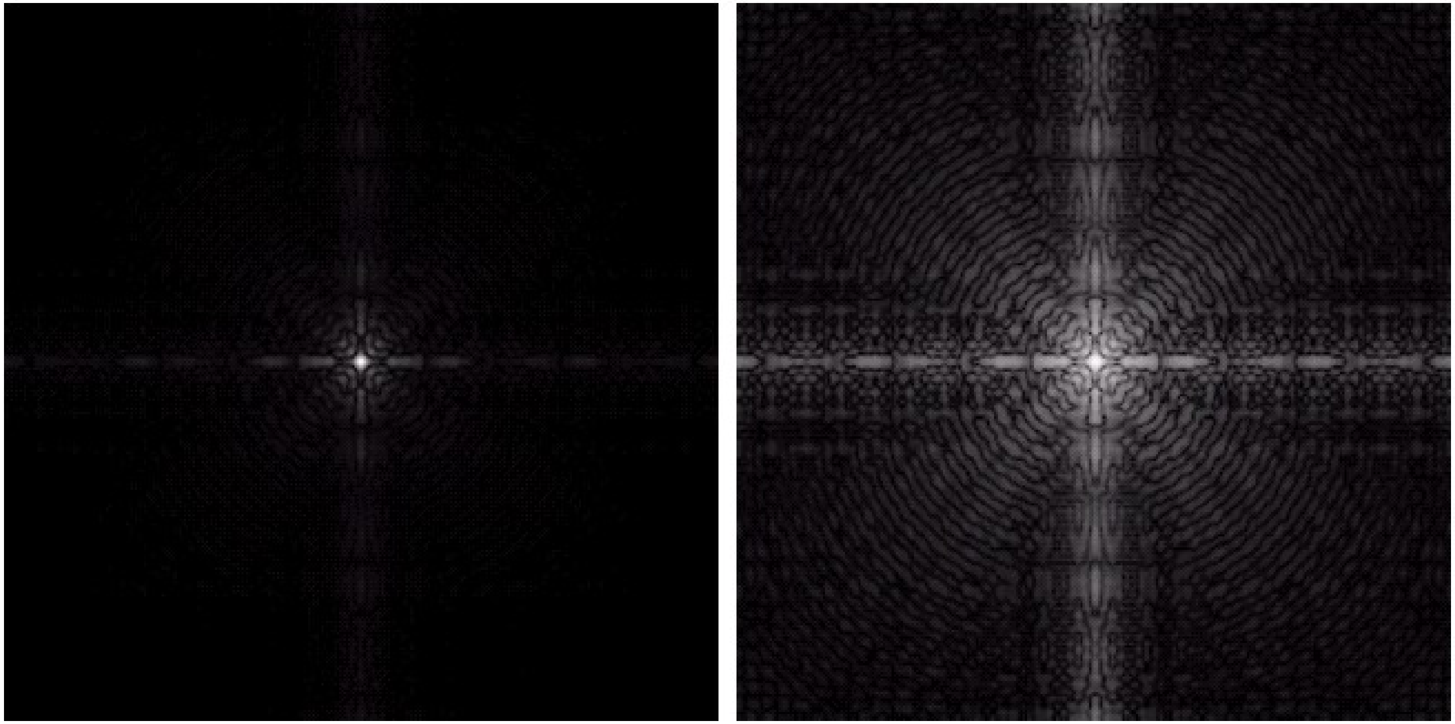

- Power-law transformations
- $$s = cr^{\gamma} \quad \text{or} \quad s = c(r+\varepsilon)^{\gamma}$$
  - $\gamma < 1$ maps a narrow range of dark input values into a wider range of output values, while $\gamma > 1$ maps a narrow range of bright input values into a wider range of output values
  - $\gamma$ : gamma, gamma correction

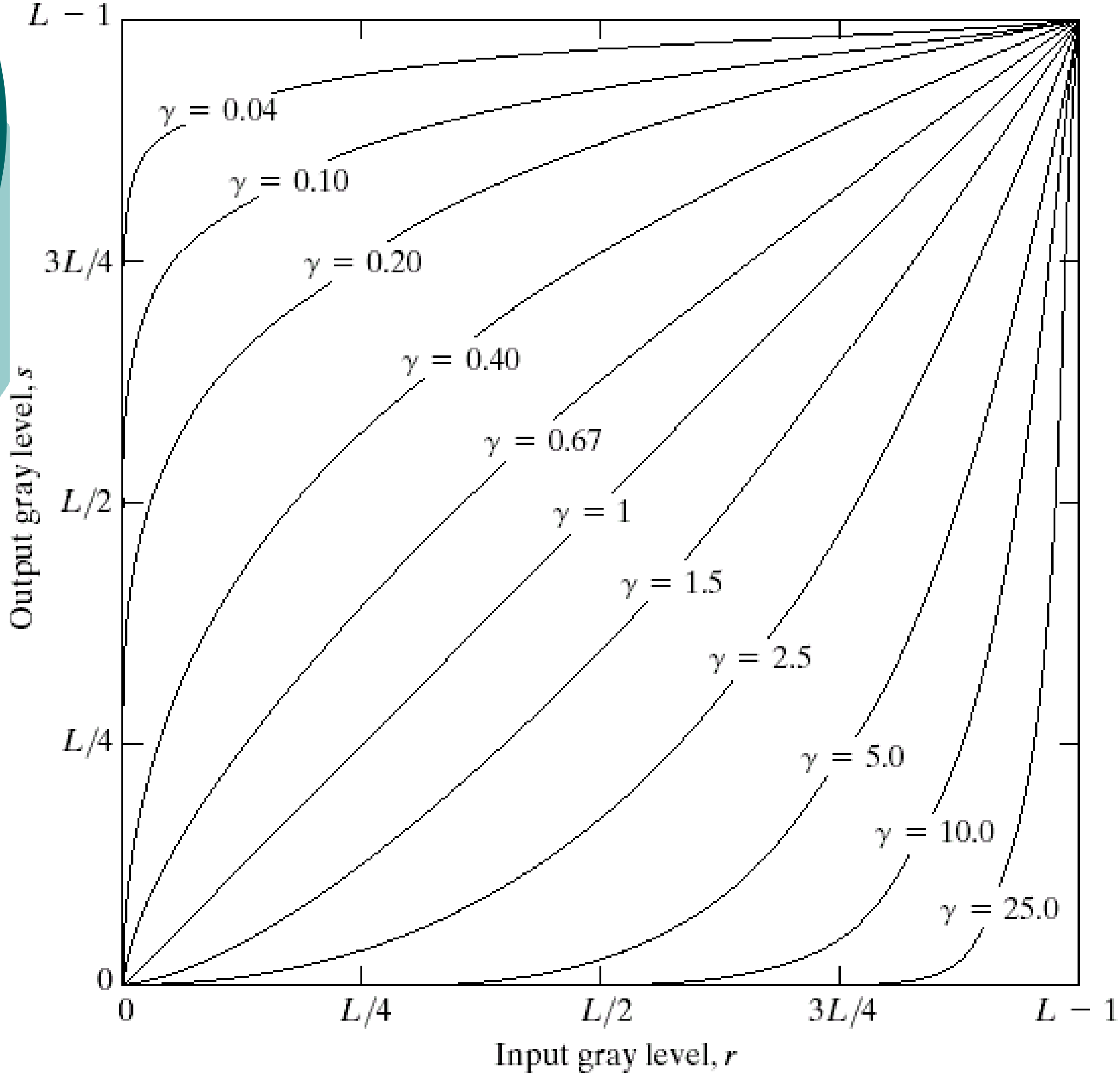


**FIGURE 3.6** Plots of the equation $s = cr^{\gamma}$ for various values of $\gamma$ ($c = 1$ in all cases).

- Monitor, $\gamma = 2.5$

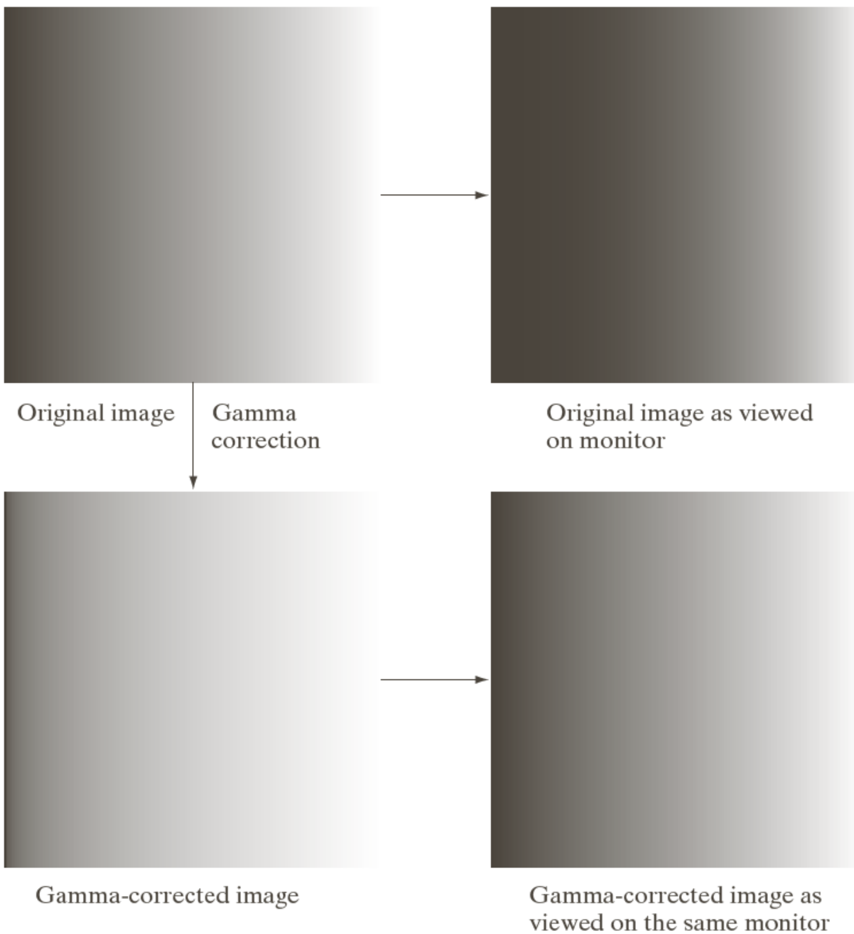


| a | b |
| --- | --- |
| c | d |

**FIGURE 3.7** (a) Intensity ramp image. (b) Image as viewed on a simulated monitor with a gamma of 2.5. (c) Gamma-corrected image. (d) Corrected image as viewed on the same monitor. Compare (d) and (a).

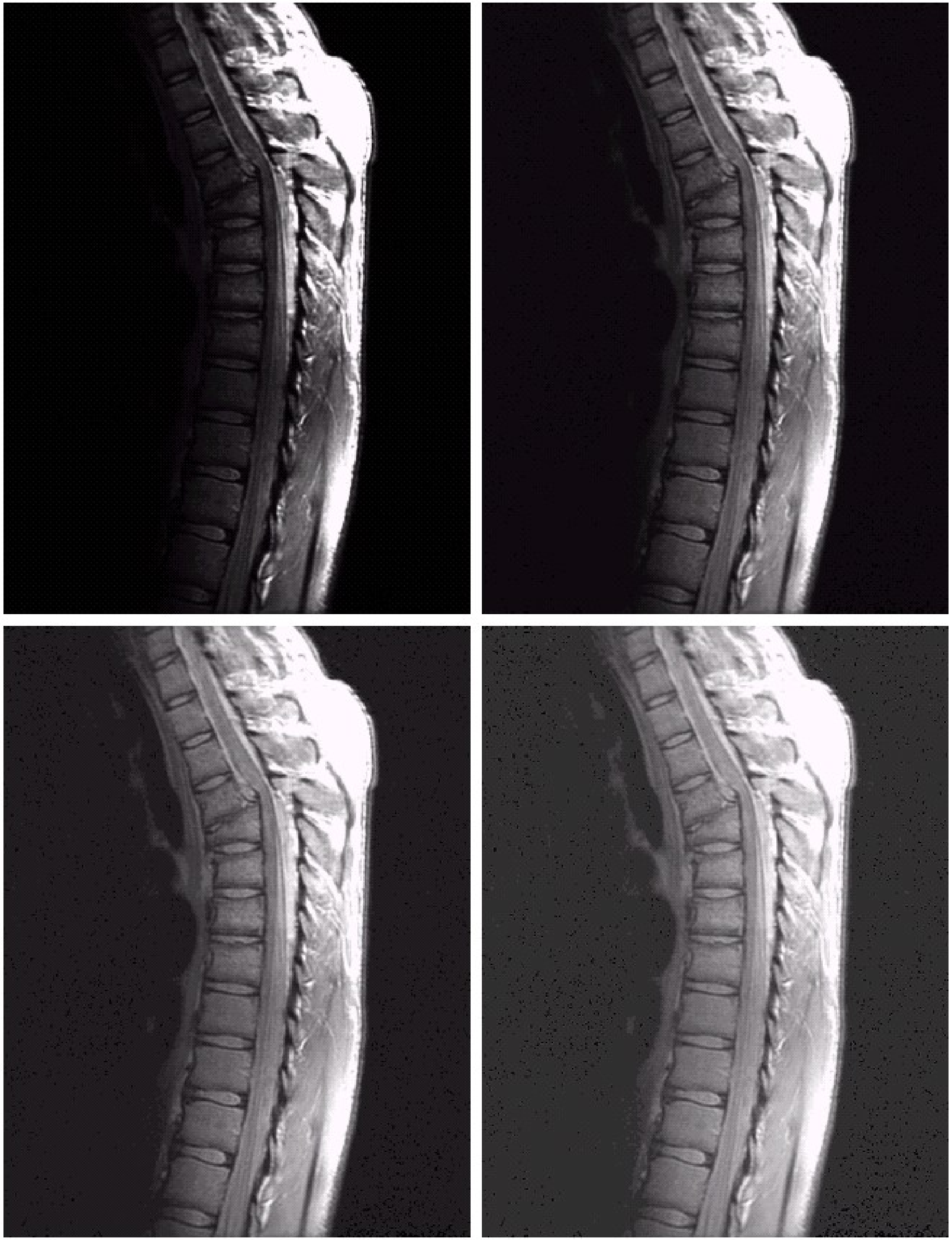

a b
c d

**FIGURE 3.8** (a) Magnetic resonance (MR) image of a fractured human spine. (b)–(d) Results of applying the transformation in Eq. (3.2-3) with $c = 1$ and $\gamma = 0.6, 0.4$, and $0.3$, respectively. (Original image for this example courtesy of Dr. David R. Pickens, Department of Radiology and Radiological Sciences, Vanderbilt University Medical Center.)

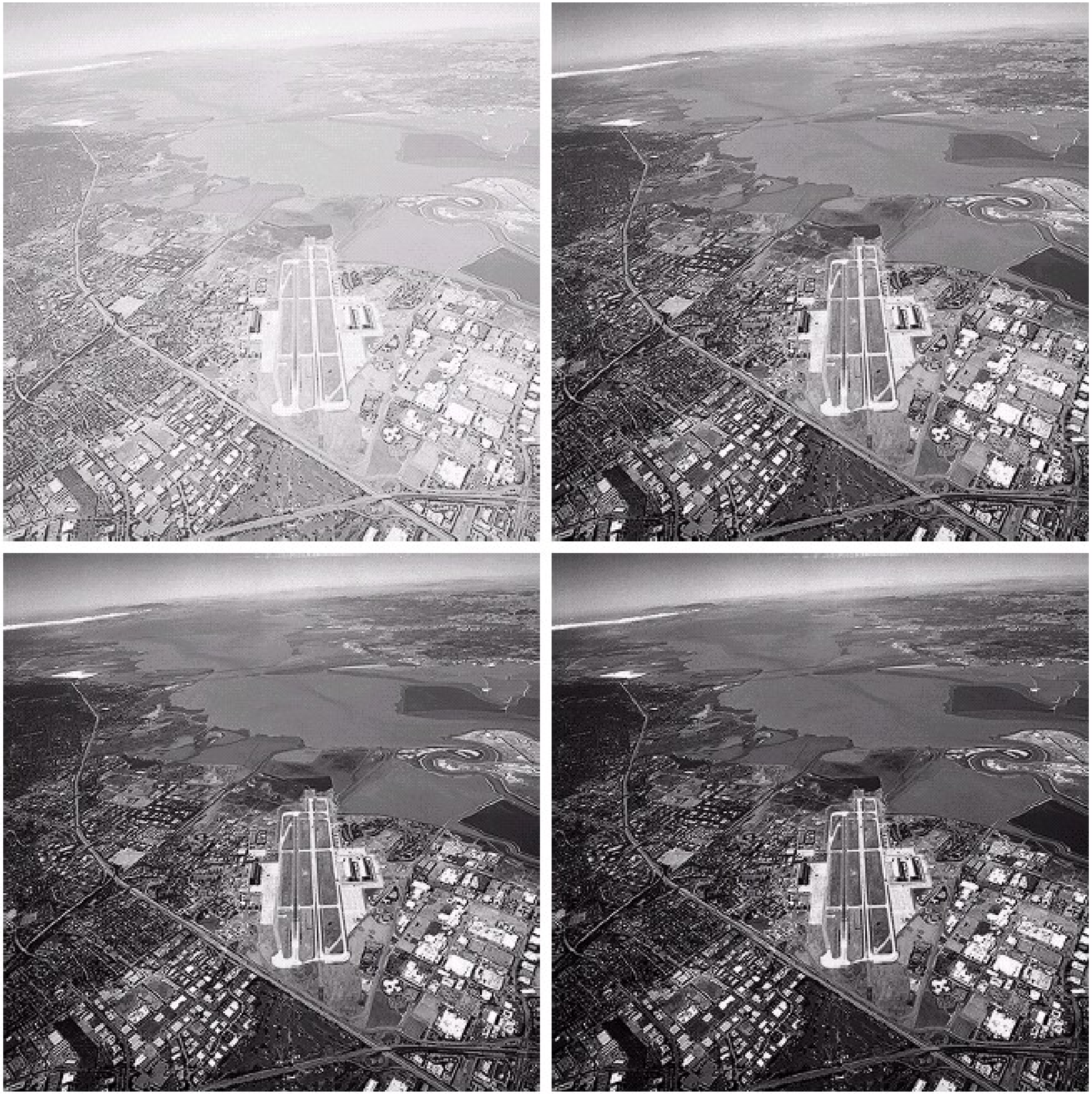

a b
c d

**FIGURE 3.9**
(a) Aerial image. (b)–(d) Results of applying the transformation in Eq. (3.2-3) with $c = 1$ and $\gamma = 3.0, 4.0,$ and $5.0$, respectively. (Original image for this example courtesy of NASA.)

- Piecewise-linear transformation functions
  - The form of piecewise functions can be arbitrarily complex

- Contrast stretching

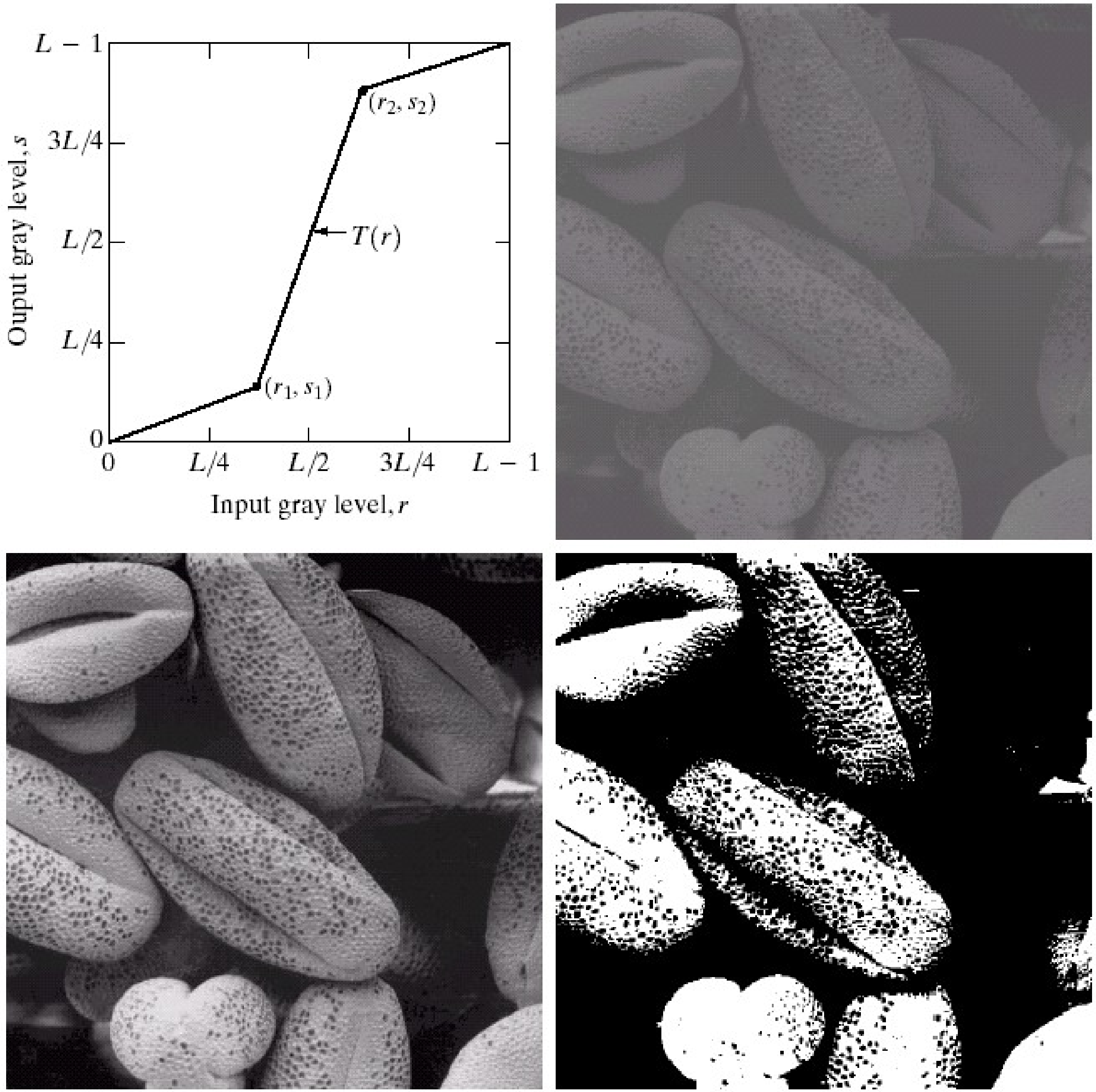


**FIGURE 3.10** Contrast stretching. (a) Form of transformation function. (b) A low-contrast image. (c) Result of contrast stretching. (d) Result of thresholding. (Original image courtesy of Dr. Roger Heady, Research School of Biological Sciences, Australian National University, Canberra, Australia.)

- Gray-level slicing

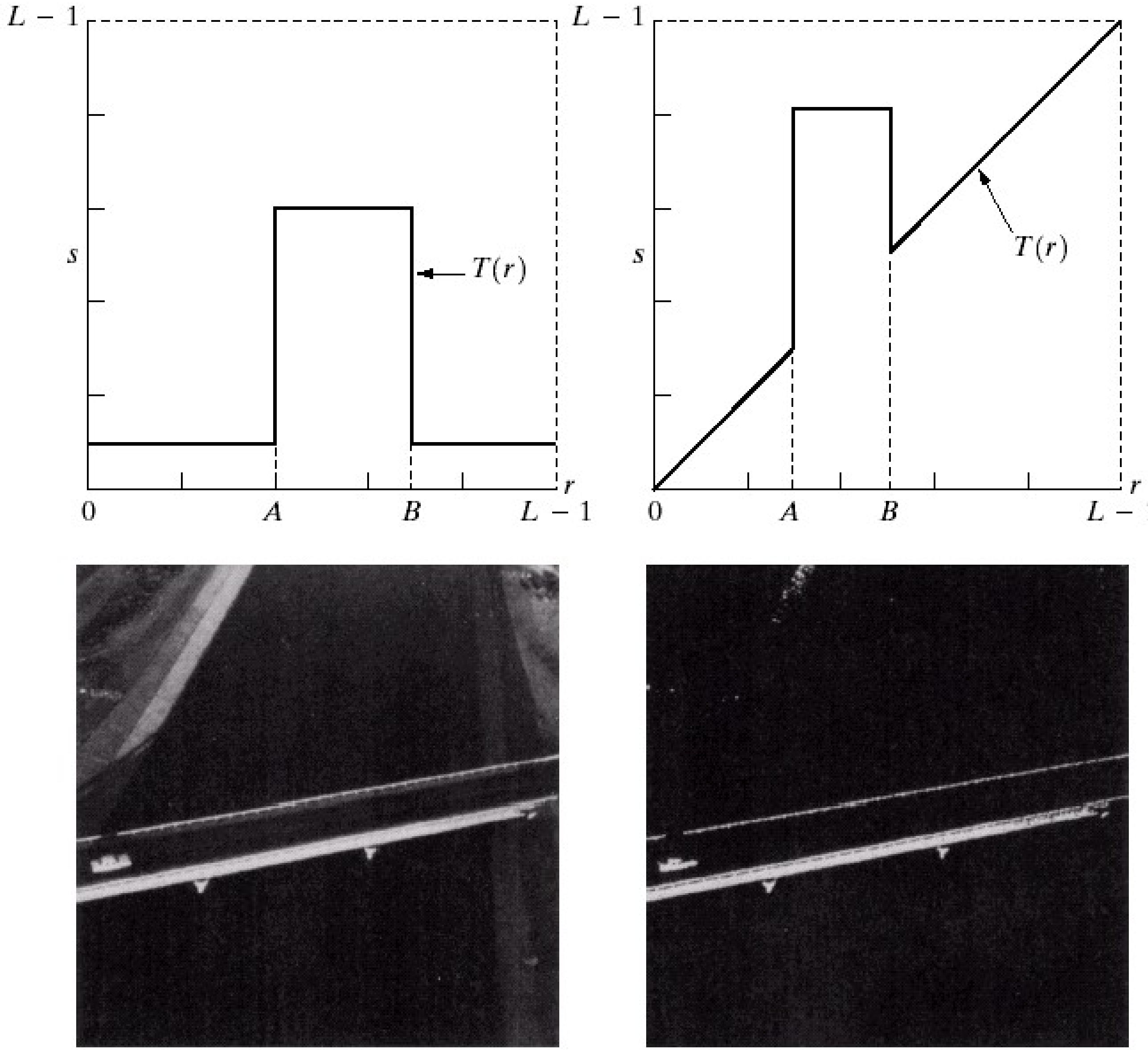


a b
c d

**FIGURE 3.11** (a) This transformation highlights range [A, B] of gray levels and reduces all others to a constant level. (b) This transformation highlights range [A, B] but preserves all other levels. (c) An image. (d) Result of using the transformation in (a).

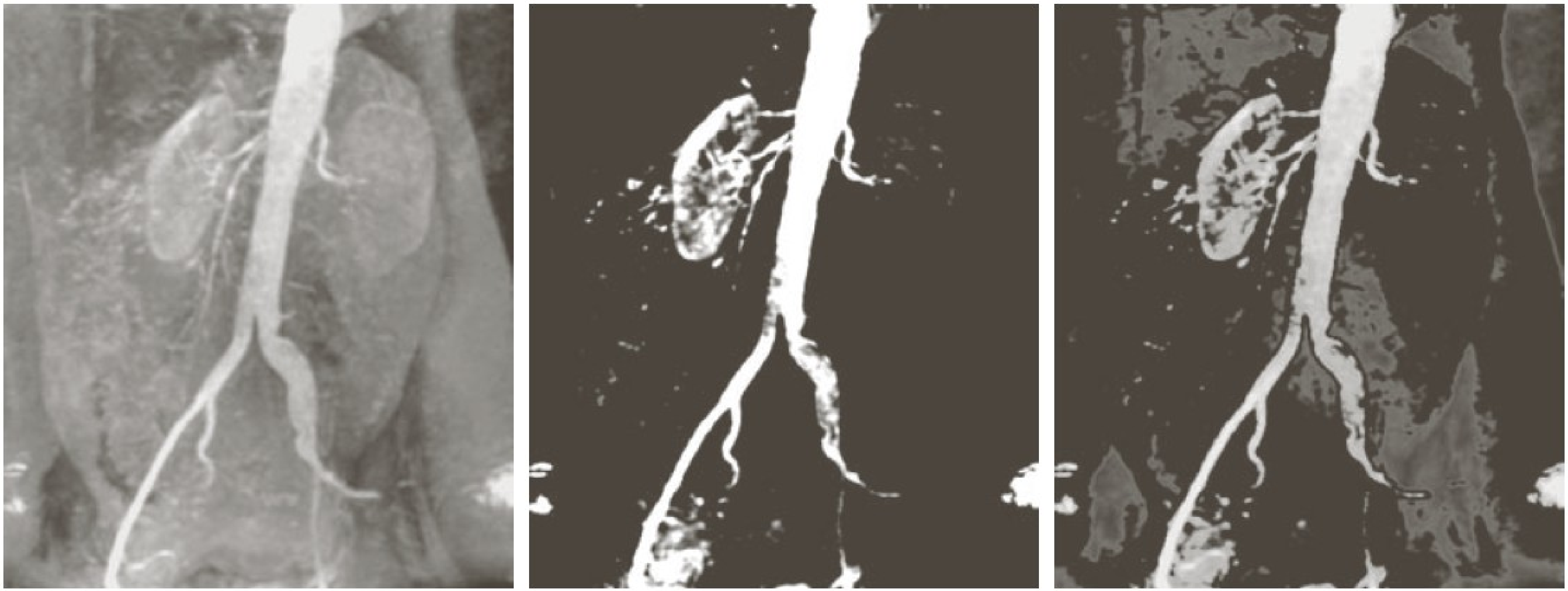

a b c

**FIGURE 3.12** (a) Aortic angiogram. (b) Result of using a slicing transformation of the type illustrated in Fig. 3.11(a), with the range of intensities of interest selected in the upper end of the gray scale. (c) Result of using the transformation in Fig. 3.11(b), with the selected area set to black, so that grays in the area of the blood vessels and kidneys were preserved. (Original image courtesy of Dr. Thomas R. Gest, University of Michigan Medical School.)

- Bit-plane slicing

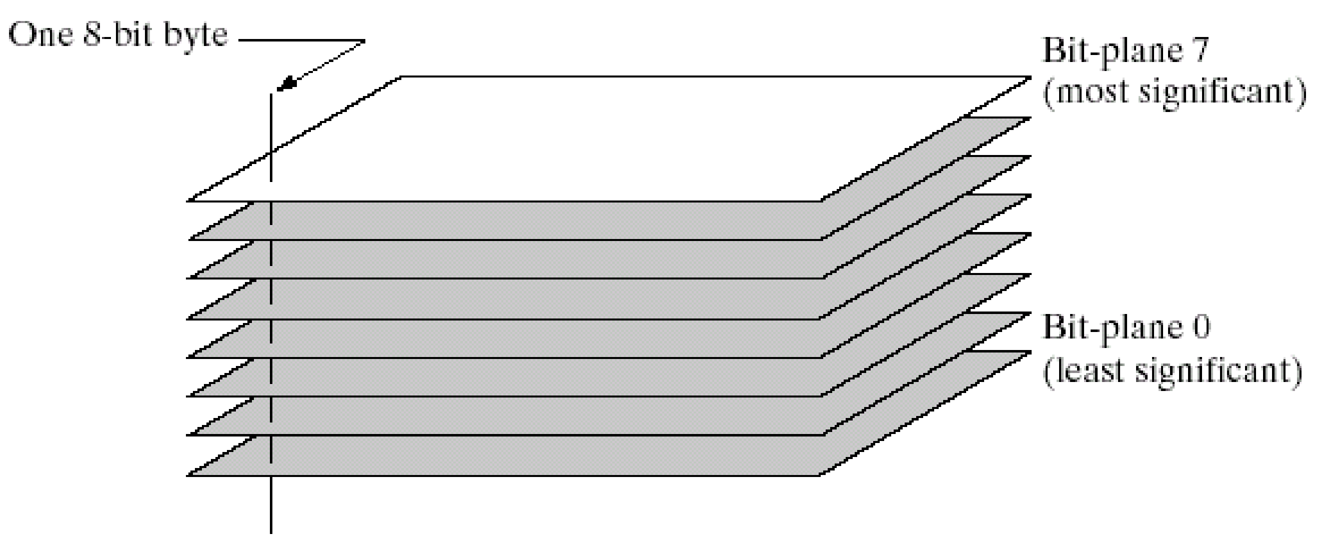


**FIGURE 3.12** Bit-plane representation of an 8-bit image.

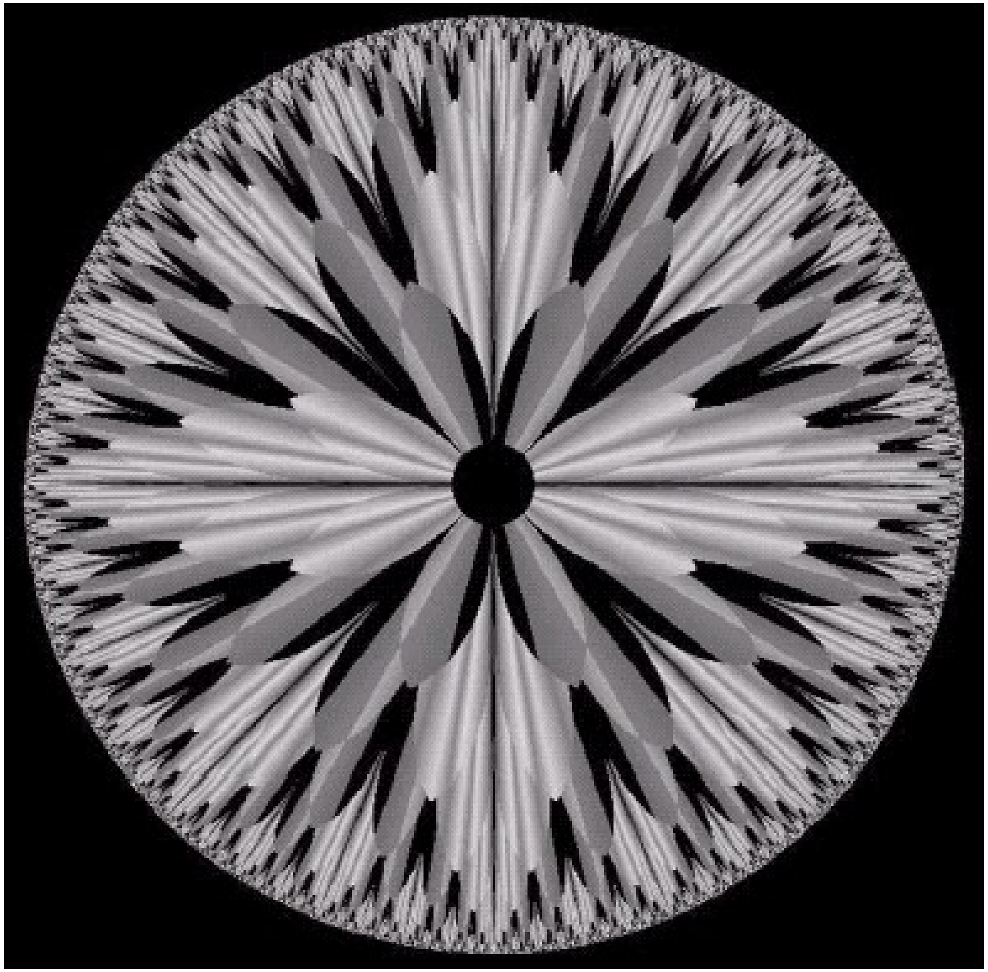

**FIGURE 3.13** An 8-bit fractal image. (A fractal is an image generated from mathematical expressions). (Courtesy of Ms. Melissa D. Binde, Swarthmore College, Swarthmore, PA.)

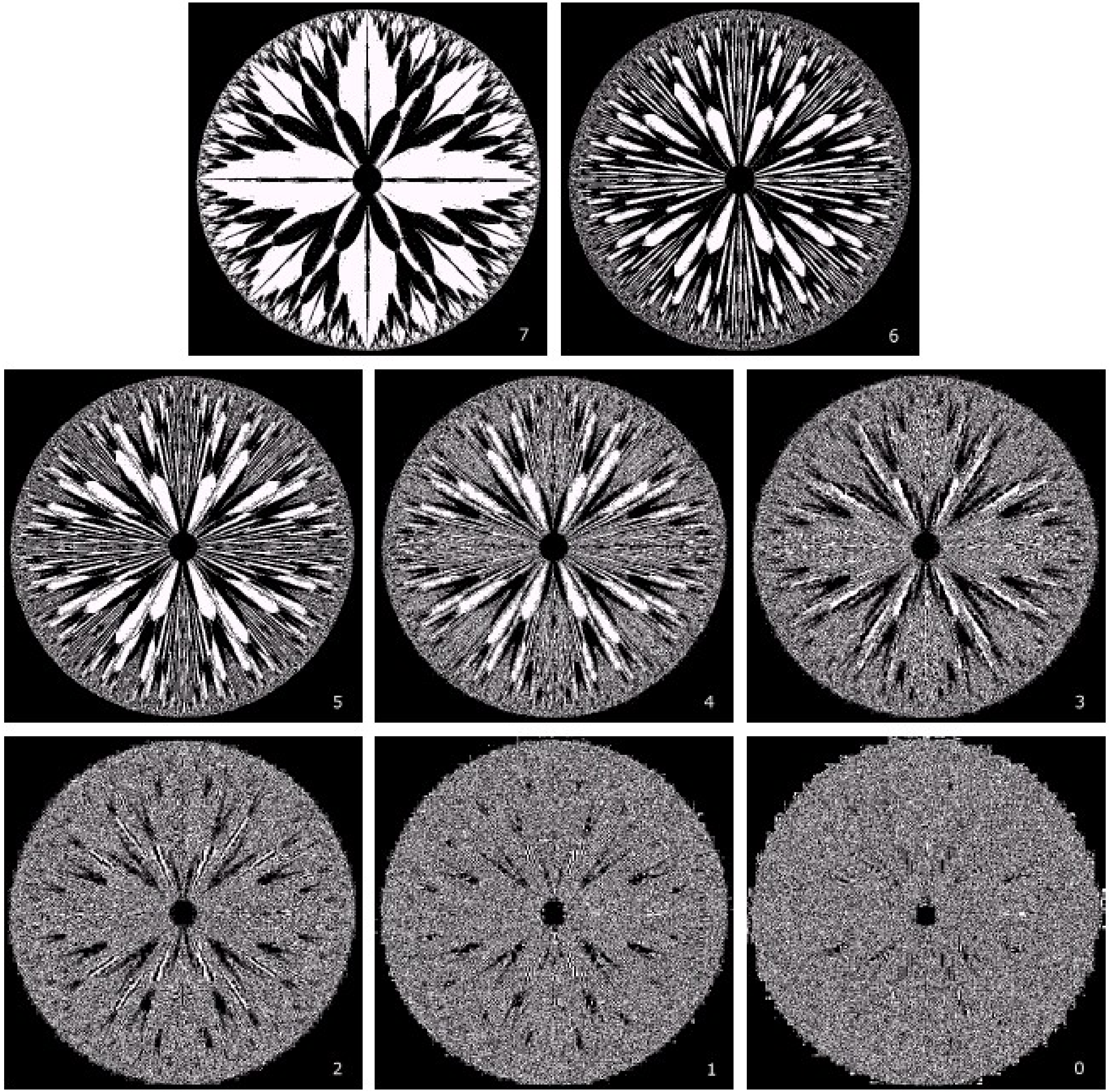


**FIGURE 3.14** The eight bit planes of the image in Fig. 3.13. The number at the bottom, right of each image identifies the bit plane.

a b c
d e f
g h i

**FIGURE 3.14** (a) An 8-bit gray-scale image of size 500 × 1192 pixels. (b) through (i) Bit planes 1 through 8, with bit plane 1 corresponding to the least significant bit. Each bit plane is a binary image.

a b c

**FIGURE 3.15** Images reconstructed using (a) bit planes 8 and 7; (b) bit planes 8, 7, and 6; and (c) bit planes 8, 7, 6, and 5. Compare (c) with Fig. 3.14(a).

# Histogram Processing

- Histogram

$$h(r_k) = n_k$$

  - where $r_k$ is the kth gray level and $n_k$ is the number of pixels in the image having gray level $r_k$
  - Normalized histogram

$$p(r_k) = n_k / n$$

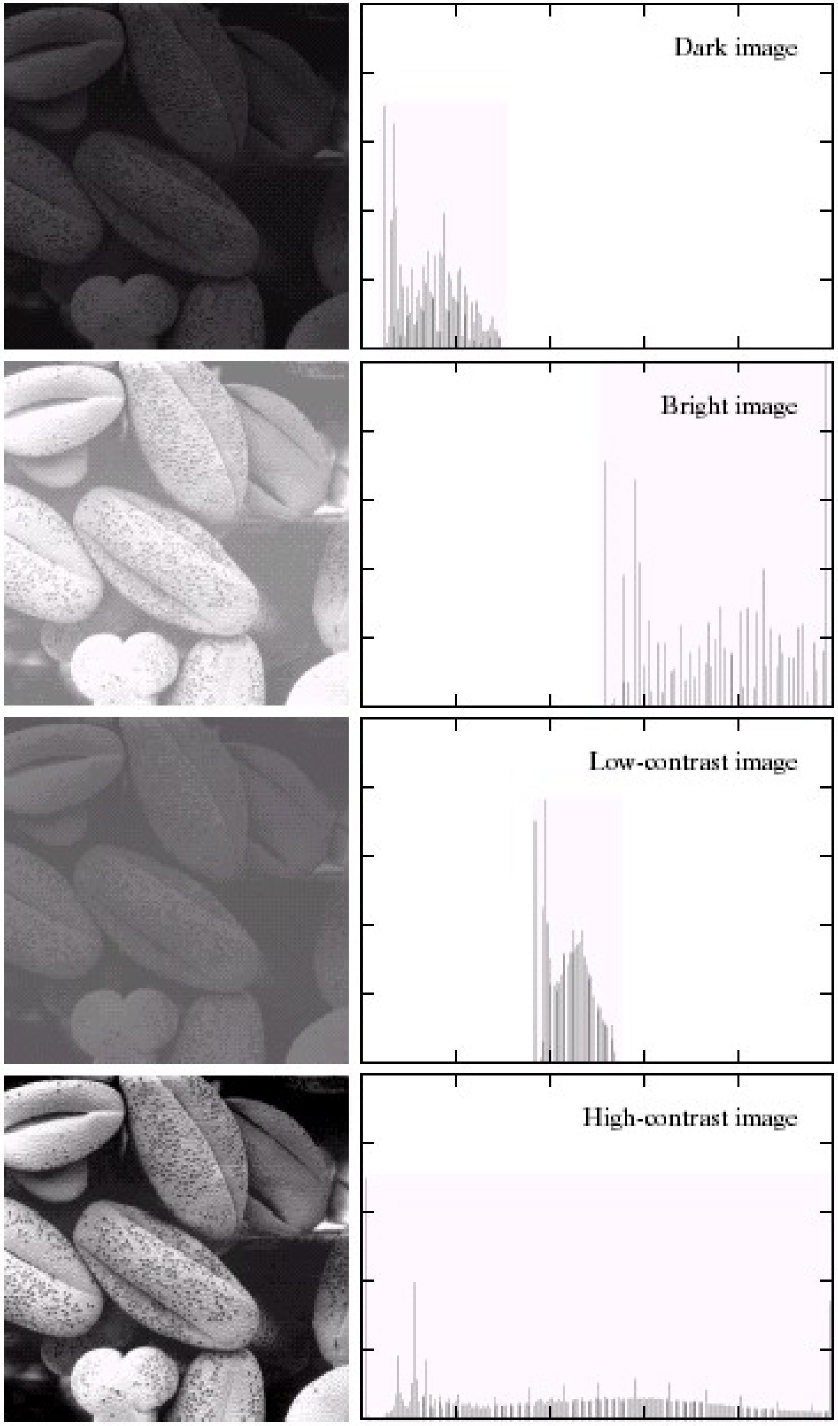
Dark image
Bright image
Low-contrast image
High-contrast image

- Histogram equalization

$$s = T(r),\ 0 \le r \le 1$$

$$r = T^{-1}(s),\ 0 \le s \le 1$$

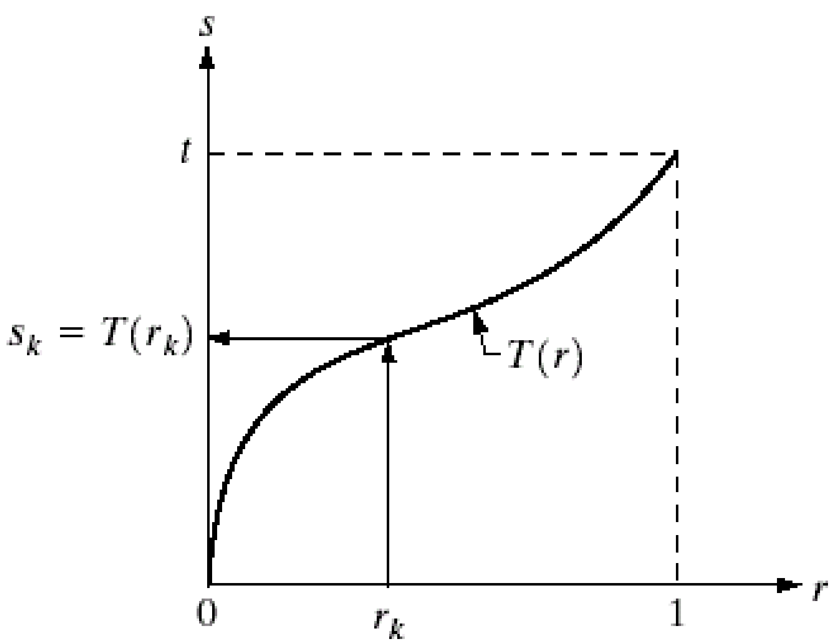


**FIGURE 3.16** A gray-level transformation function that is both single valued and monotonically increasing.

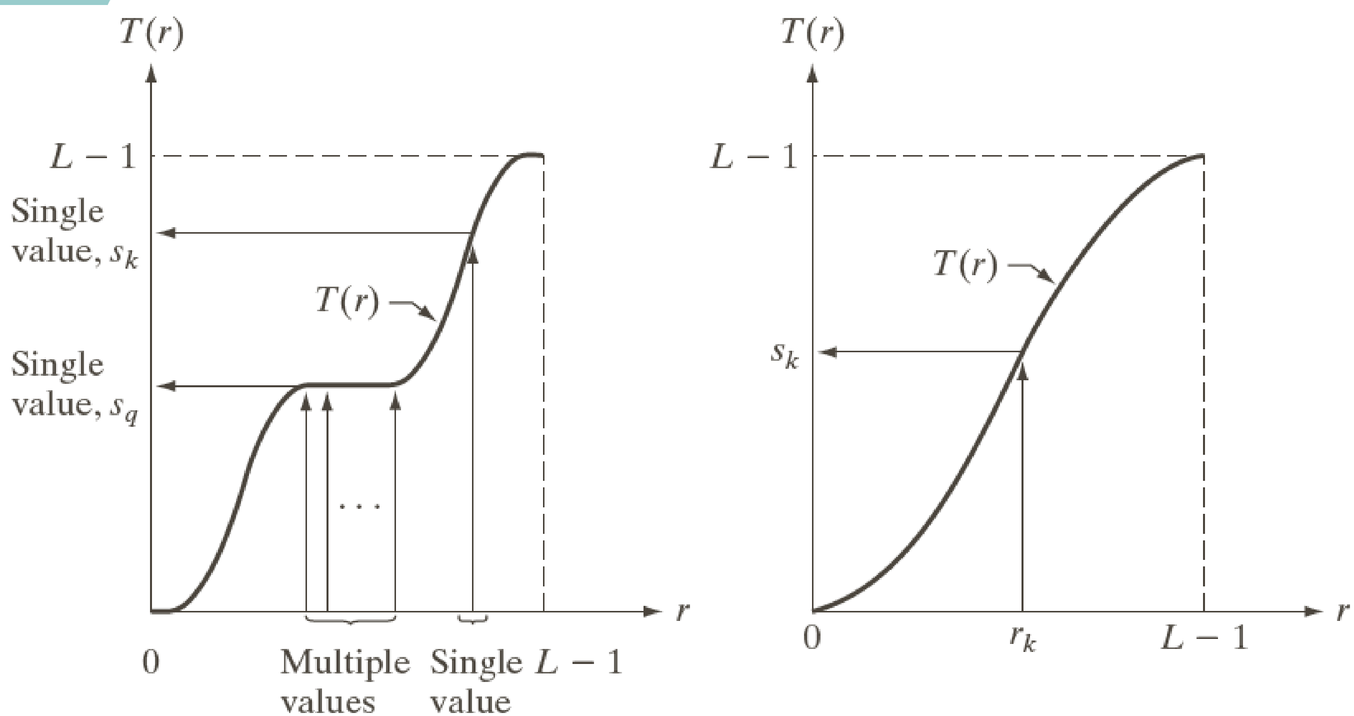


a b

**FIGURE 3.17** (a) Monotonically increasing function, showing how multiple values can map to a single value. (b) Strictly monotonically increasing function. This is a one-to-one mapping, both ways.

- Probability density functions (PDF)

$$p_s(s) = p_r(r)\left|\frac{dr}{ds}\right|$$

$$s = T(r) = (L-1)\int_0^r p_r(w)\,dw$$

$$\frac{ds}{dr} = \frac{dT(r)}{dr} = (L-1)\frac{d}{dr}\left[\int_0^r p_r(w)\,dw\right] = (L-1)\,p_r(r)$$

$$\Rightarrow \quad p_s(s) = \frac{1}{L-1}$$

$$s_k = T(r_k) = (L-1)\sum_{j=0}^{k} p_r(r_j) = (L-1)\sum_{j=0}^{k} \frac{n_j}{n}, \quad k = 0,1,2,\ldots,L-1$$

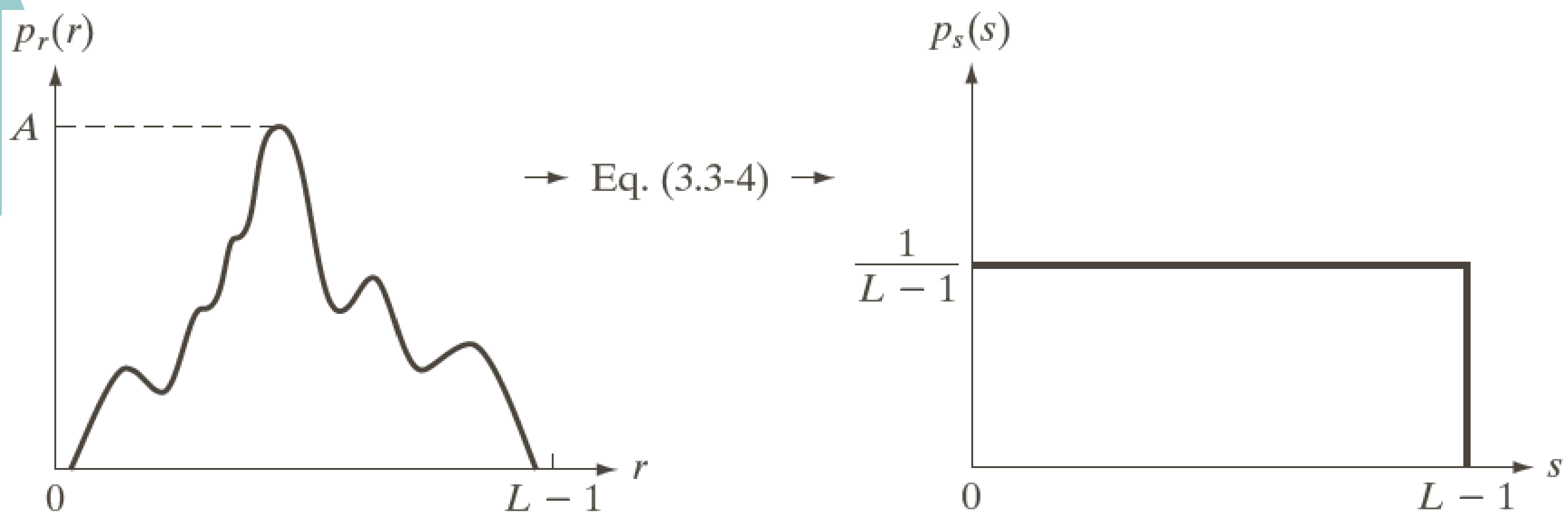


a b

**FIGURE 3.18** (a) An arbitrary PDF. (b) Result of applying the transformation in Eq. (3.3-4) to all intensity levels, $r$. The resulting intensities, $s$, have a uniform PDF, independently of the form of the PDF of the $r$'s.

| $r_k$ | $n_k$ | $p_r(r_k) = n_k/MN$ |
|---|---|---|
| $r_0 = 0$ | 790 | 0.19 |
| $r_1 = 1$ | 1023 | 0.25 |
| $r_2 = 2$ | 850 | 0.21 |
| $r_3 = 3$ | 656 | 0.16 |
| $r_4 = 4$ | 329 | 0.08 |
| $r_5 = 5$ | 245 | 0.06 |
| $r_6 = 6$ | 122 | 0.03 |
| $r_7 = 7$ | 81 | 0.02 |

**TABLE 3.1** Intensity distribution and histogram values for a 3-bit, $64 \times 64$ digital image.

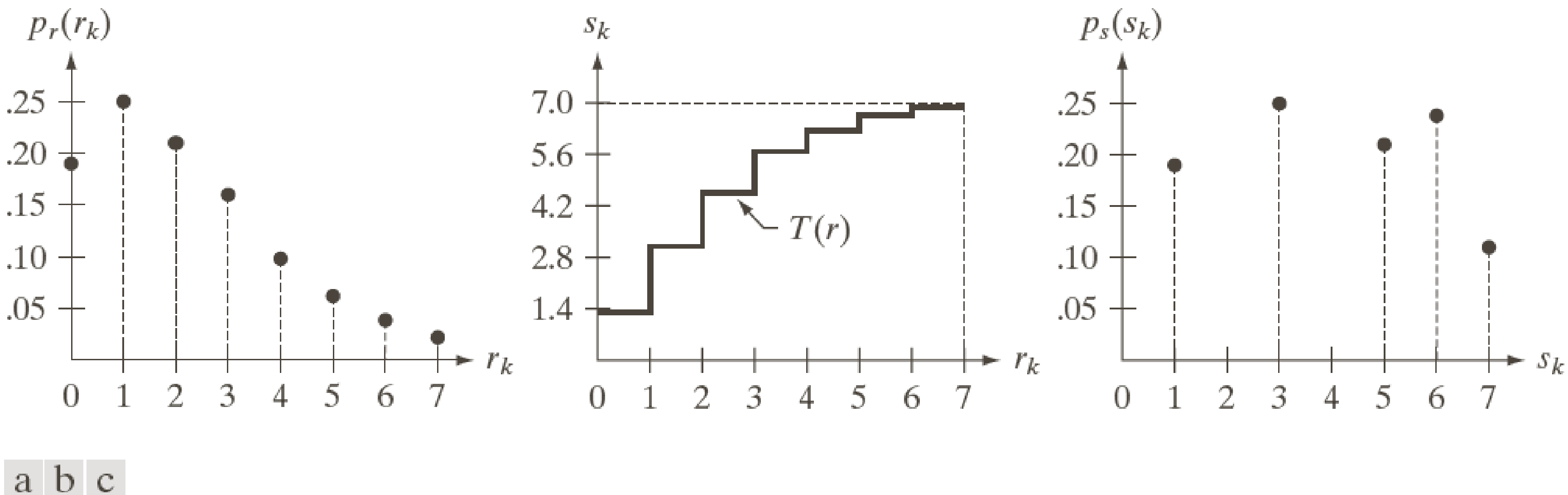


**FIGURE 3.19** Illustration of histogram equalization of a 3-bit (8 intensity levels) image. (a) Original histogram. (b) Transformation function. (c) Equalized histogram.

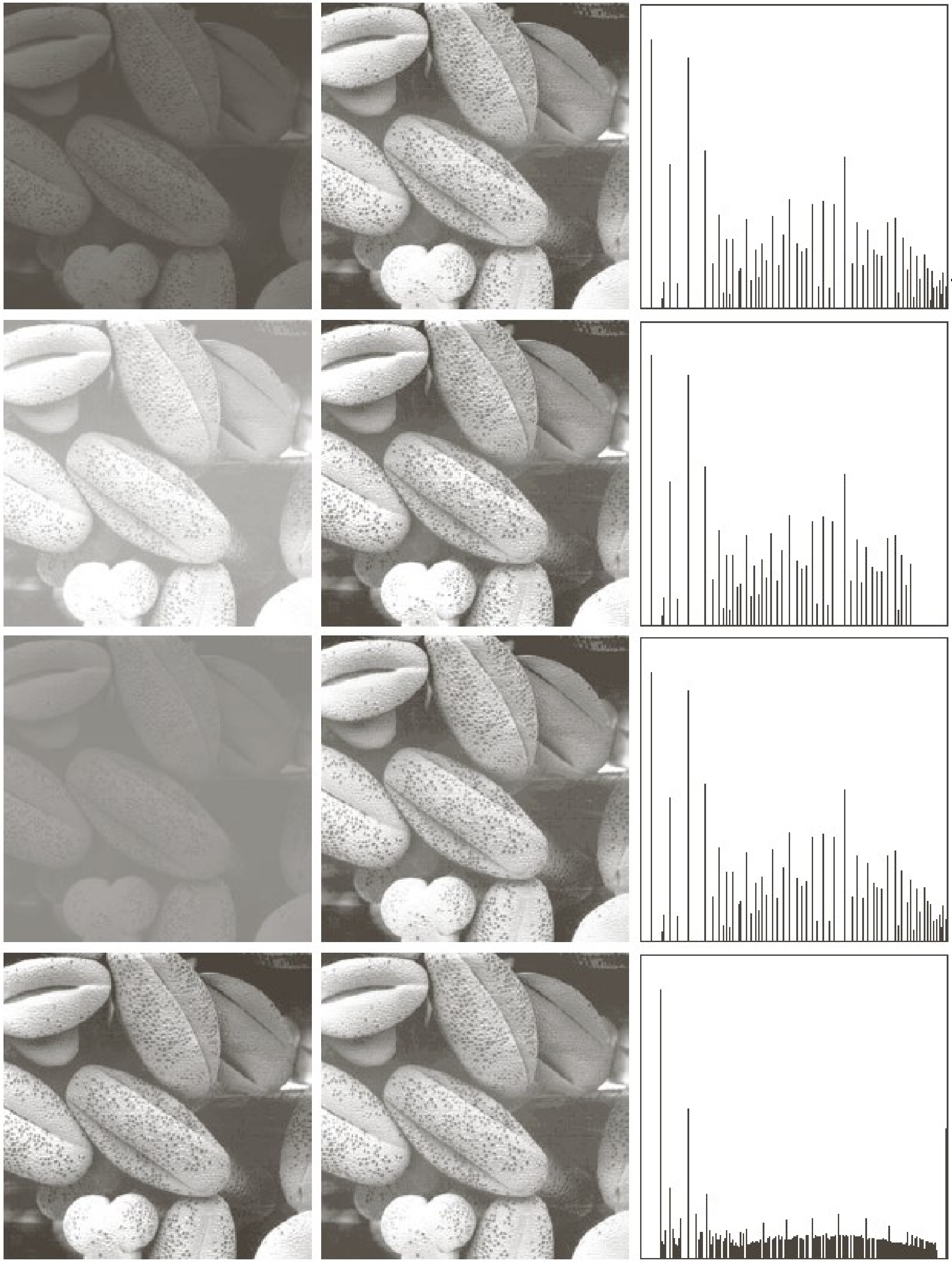

**FIGURE 3.18** Transformation functions (1) through (4) were obtained from the histograms of the images in Fig.3.17(a), using Eq. (3.3-8).

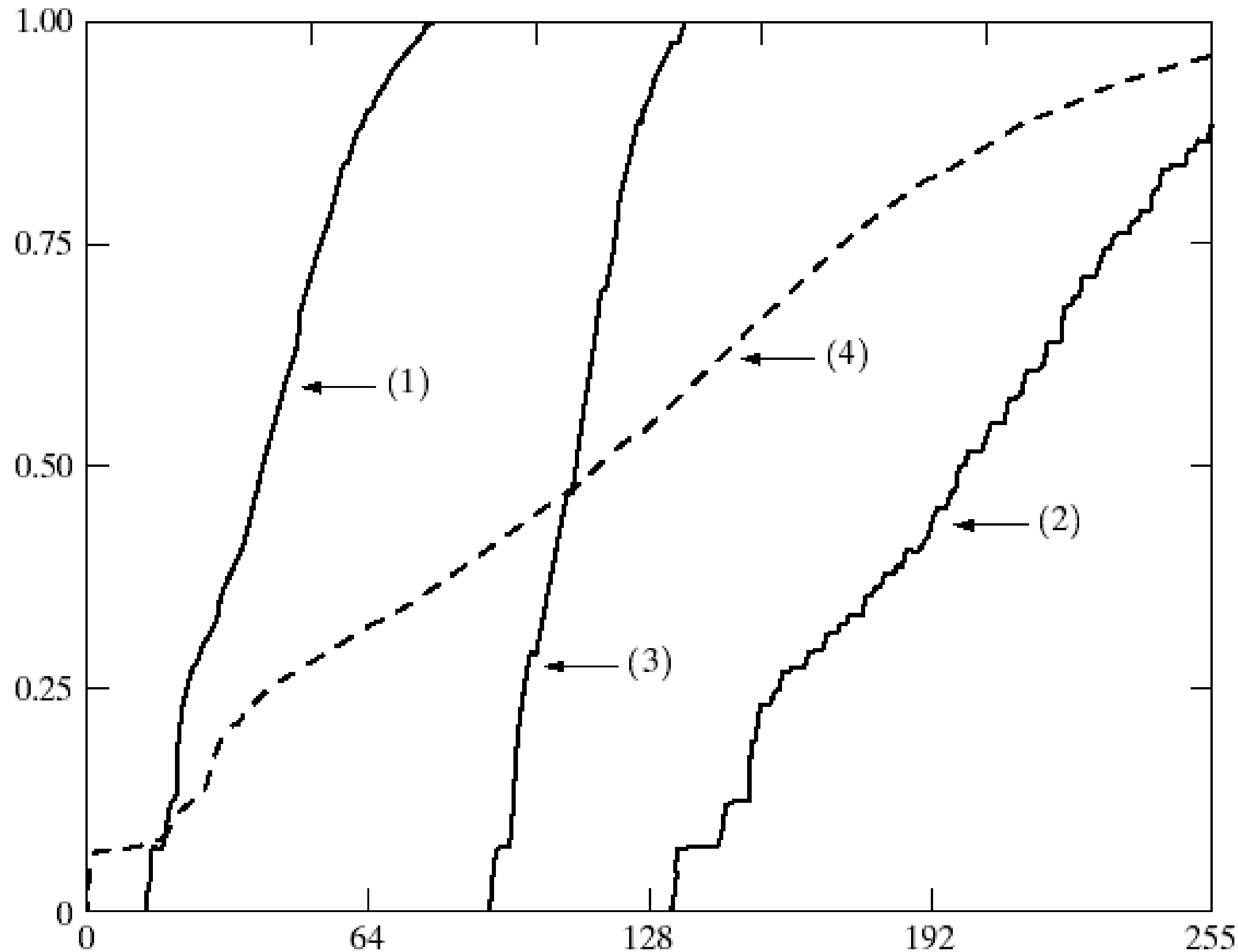

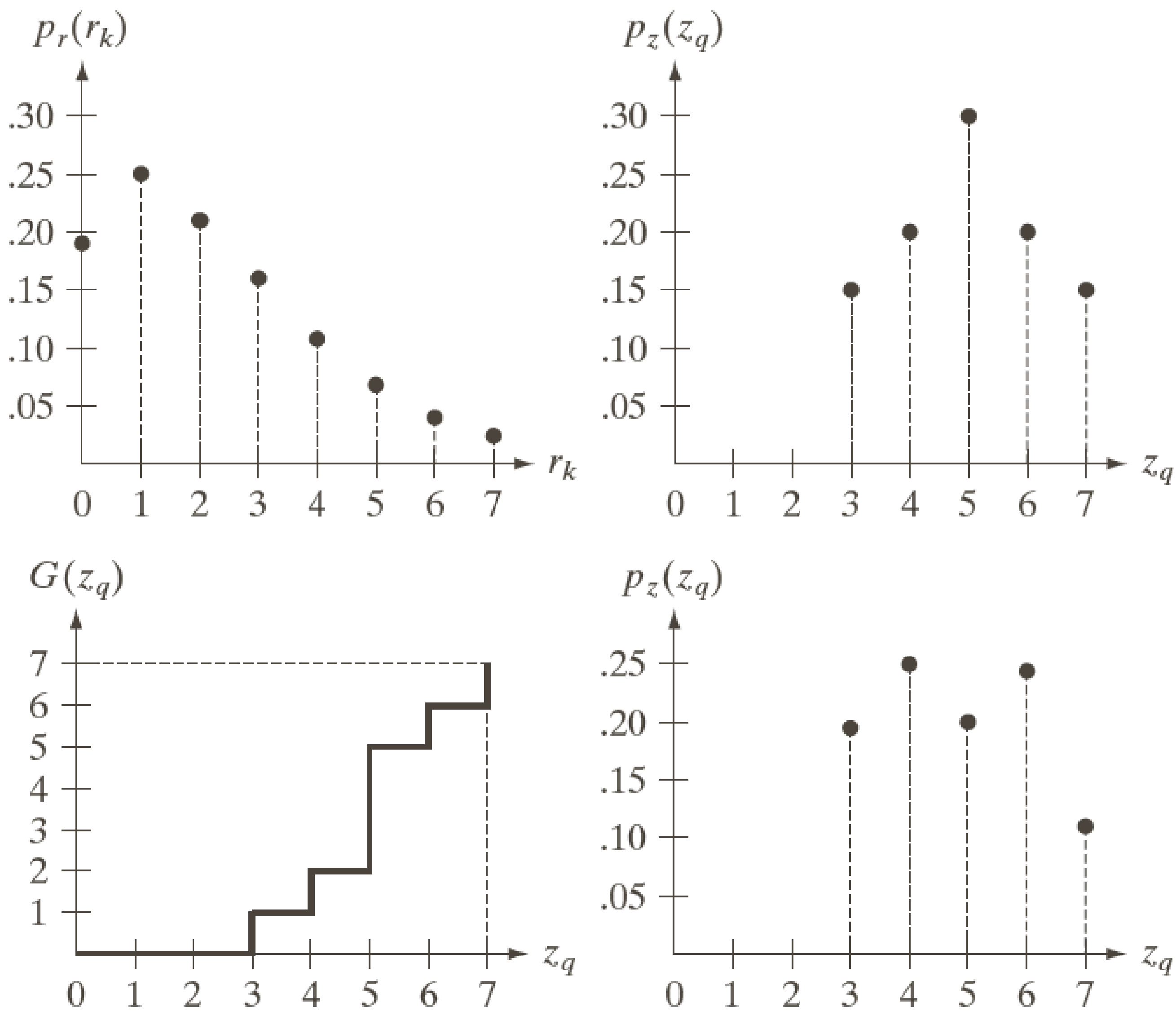


| | |
|---|---|
| a | b |
| c | d |

**FIGURE 3.22**
(a) Histogram of a 3-bit image. (b) Specified histogram.
(c) Transformation function obtained from the specified histogram.
(d) Result of performing histogram specification. Compare (b) and (d).

- Histogram matching (specification)

$$s = T(r) = (L-1)\int_0^r p_r(w)\,dw$$

$$G(z) = (L-1)\int_0^z p_z(t)\,dt = s$$

$$z = G^{-1}(s) = G^{-1}[T(r)]$$

$\Rightarrow$ $p_z(z)$ is the desired PDF

$$s_k = T(r_k) = (L-1)\sum_{j=0}^{k} p_r(r_j) = (L-1)\sum_{j=0}^{k} \frac{n_j}{n}, \quad k = 0,1,2,\ldots,L-1$$

$$v_k = G(z_k) = (L-1)\sum_{i=0}^{k} p_z(z_i) = s_k, \quad k = 0,1,2,\ldots,L-1$$

$$\Rightarrow \quad z_k = G^{-1}[T(r_k)], \quad k = 0,1,2,\ldots,L-1$$

a b
c

**FIGURE 3.19**
(a) Graphical interpretation of mapping from $r_k$ to $s_k$ via $T(r)$.
(b) Mapping of $z_q$ to its corresponding value $v_q$ via $G(z)$.
(c) Inverse mapping from $s_k$ to its corresponding value of $z_k$.

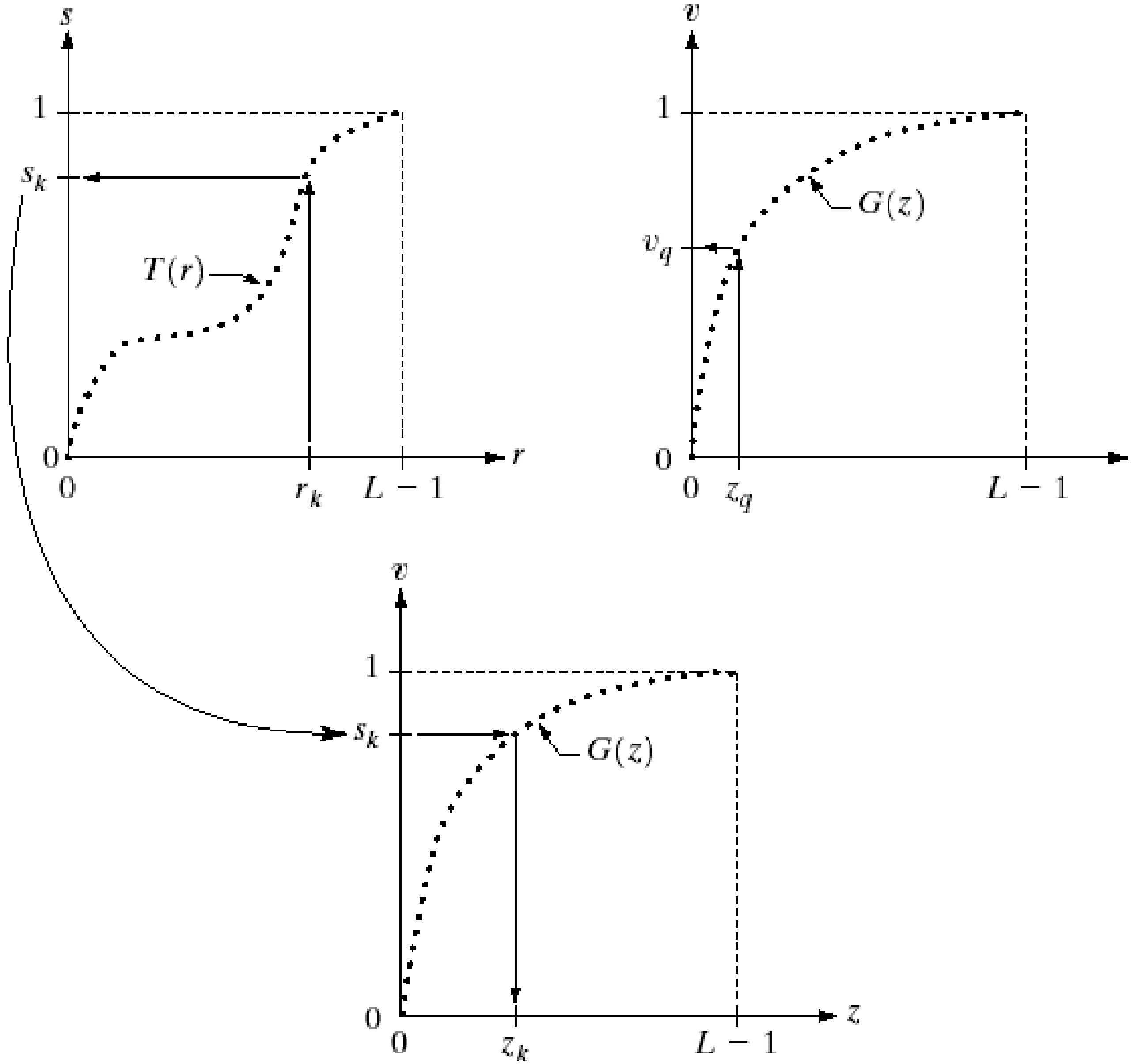

- Histogram matching
  - Obtain the histogram of the given image, T(r)
  - Precompute a mapped level $s_k$ for each level $r_k$
  - Obtain the transformation function G from the given $p_z(z)$
  - Precompute $z_k$ for each value of $s_k$
  - Map $r_k$ to its corresponding level $s_k$ ; then map level $s_k$ into the final level $z_k$

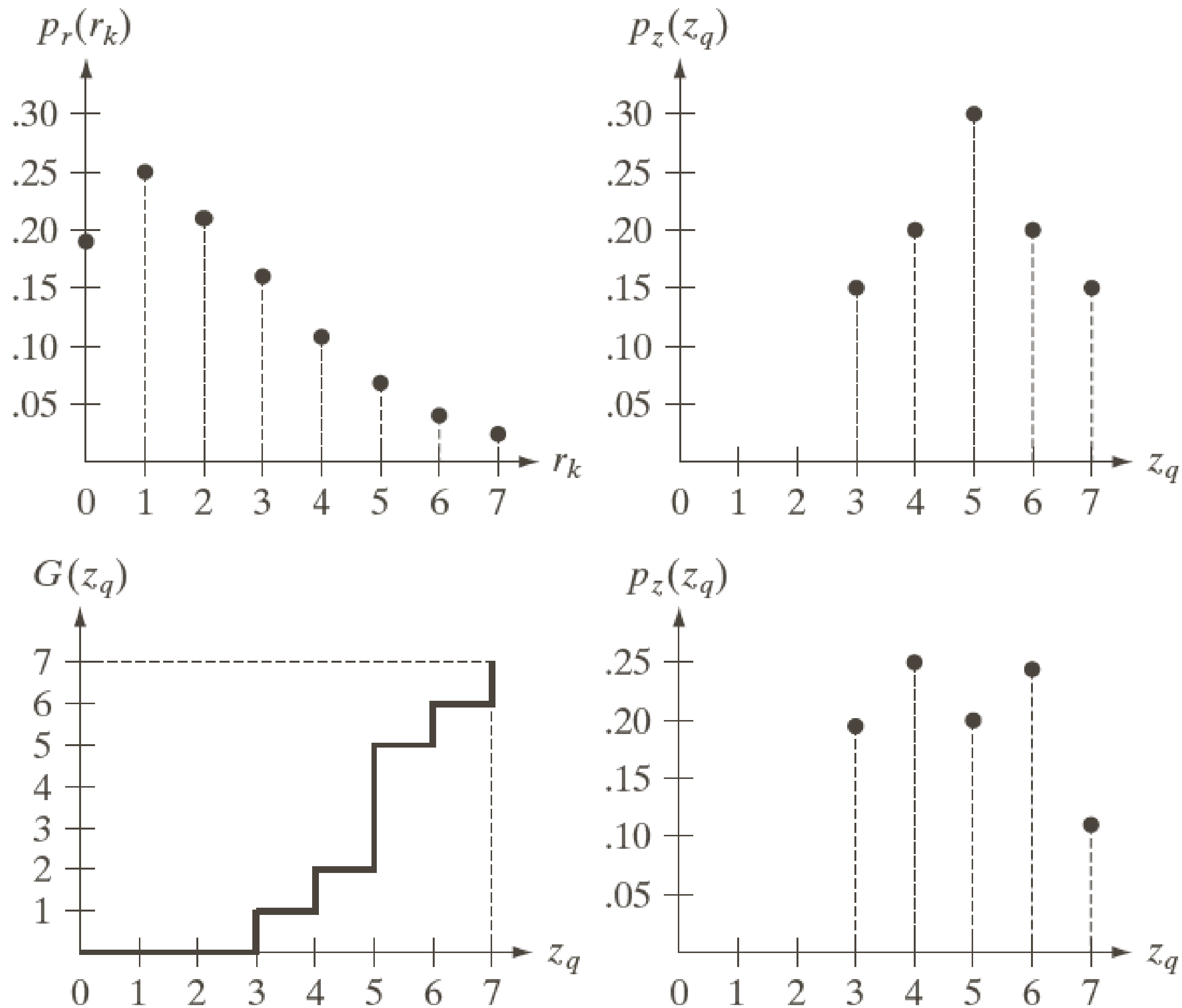


| | |
|---|---|
| a | b |
| c | d |

**FIGURE 3.22**
(a) Histogram of a 3-bit image. (b) Specified histogram. (c) Transformation function obtained from the specified histogram. (d) Result of performing histogram specification. Compare (b) and (d).

| $z_q$ | Specified $p_z(z_q)$ | Actual $p_z(z_k)$ |
|---|---|---|
| $z_0 = 0$ | 0.00 | 0.00 |
| $z_1 = 1$ | 0.00 | 0.00 |
| $z_2 = 2$ | 0.00 | 0.00 |
| $z_3 = 3$ | 0.15 | 0.19 |
| $z_4 = 4$ | 0.20 | 0.25 |
| $z_5 = 5$ | 0.30 | 0.21 |
| $z_6 = 6$ | 0.20 | 0.24 |
| $z_7 = 7$ | 0.15 | 0.11 |

**TABLE 3.2**
Specified and actual histograms (the values in the third column are from the computations performed in the body of Example 3.8).

| $z_q$ | $G(z_q)$ |
|---|---|
| $z_0 = 0$ | 0 |
| $z_1 = 1$ | 0 |
| $z_2 = 2$ | 0 |
| $z_3 = 3$ | 1 |
| $z_4 = 4$ | 2 |
| $z_5 = 5$ | 5 |
| $z_6 = 6$ | 6 |
| $z_7 = 7$ | 7 |

**TABLE 3.3**
All possible values of the transformation function $G$ scaled, rounded, and ordered with respect to $z$.

| $s_k$ | $\rightarrow$ | $z_q$ |
|---|---|---|
| 1 | $\rightarrow$ | 3 |
| 3 | $\rightarrow$ | 4 |
| 5 | $\rightarrow$ | 5 |
| 6 | $\rightarrow$ | 6 |
| 7 | $\rightarrow$ | 7 |

**TABLE 3.4**
Mappings of all the values of $s_k$ into corresponding values of $z_q$.

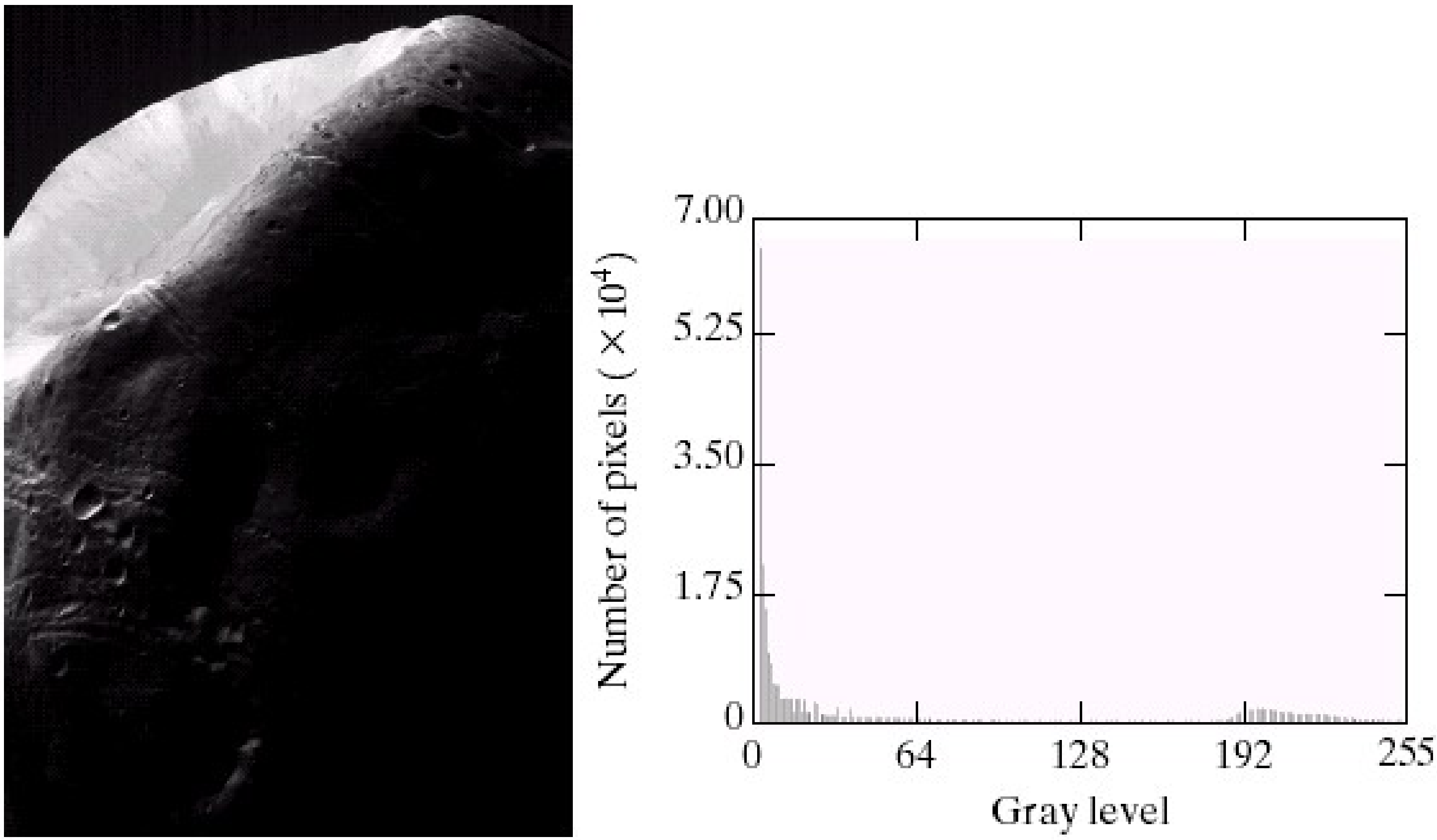


a b

**FIGURE 3.20** (a) Image of the Mars moon Photos taken by NASA's *Mars Global Surveyor*. (b) Histogram. (Original image courtesy of NASA.)

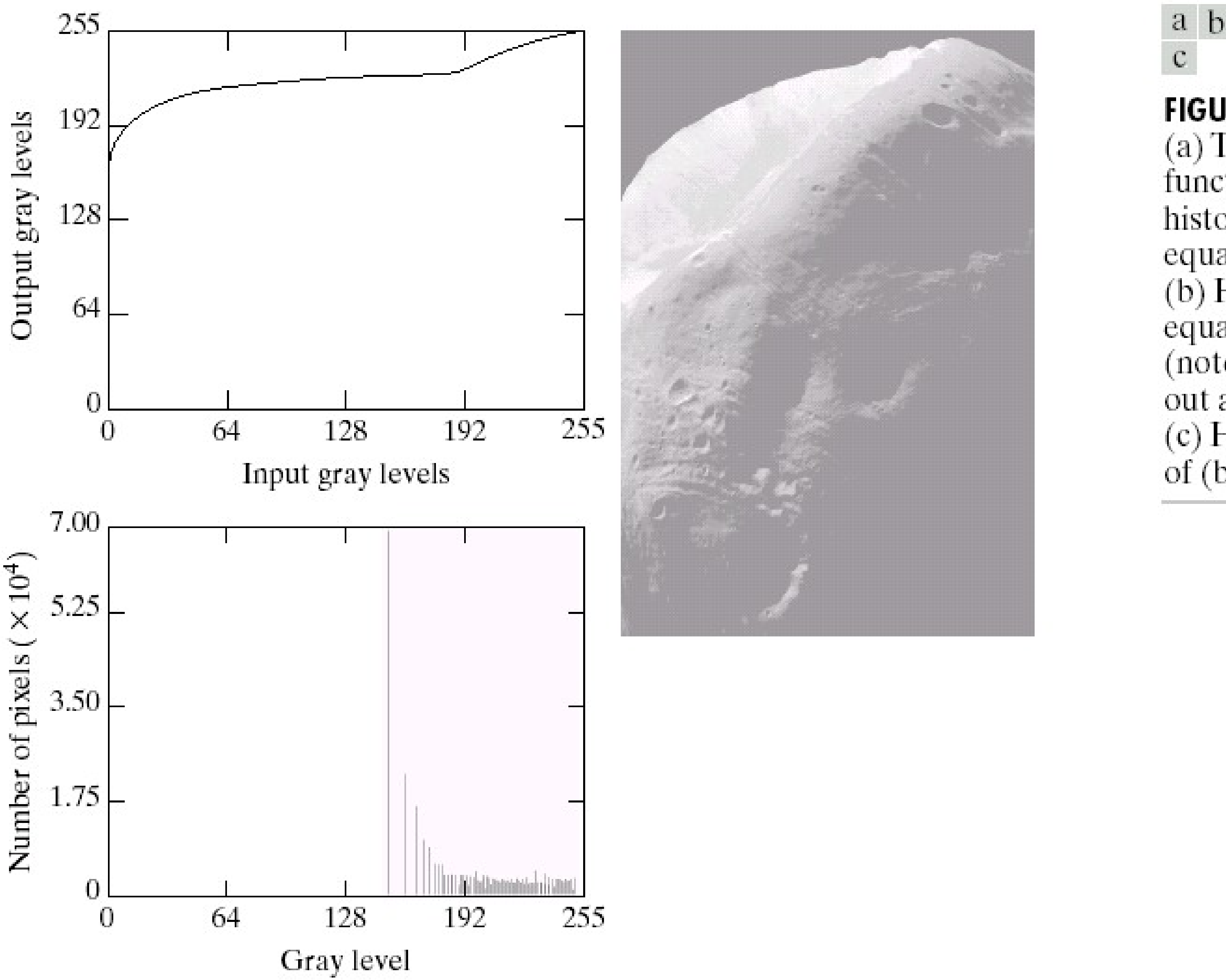


**FIGURE 3.21** (a) Transformation function for histogram equalization. (b) Histogram-equalized image (note the washed-out appearance). (c) Histogram of (b).

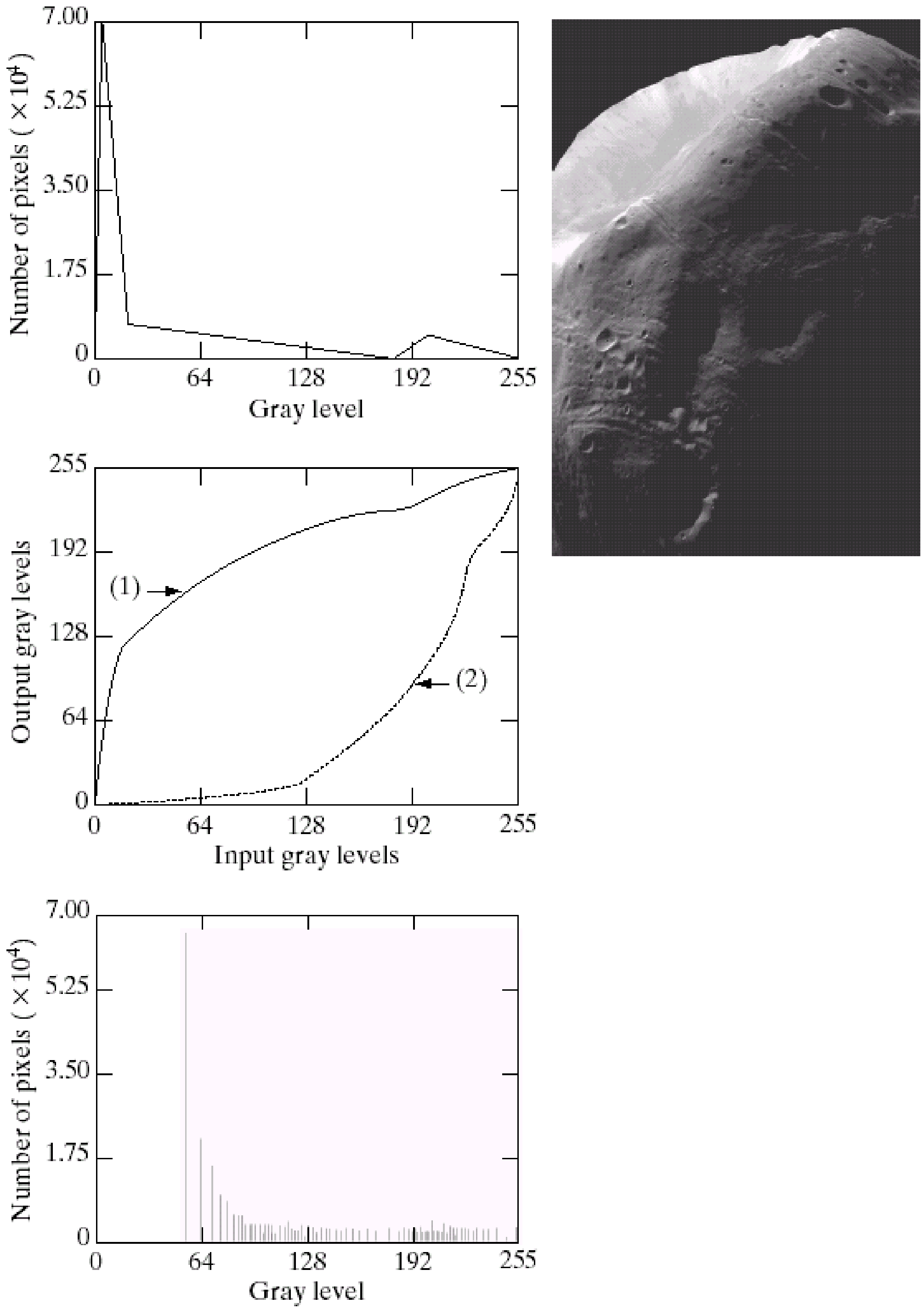


a c
b
d

**FIGURE 3.22**
(a) Specified histogram.
(b) Curve (1) is from Eq. (3.3-14), using the histogram in (a); curve (2) was obtained using the iterative procedure in Eq. (3.3-17).
(c) Enhanced image using mappings from curve (2).
(d) Histogram of (c).

- Local enhancement
  - Histogram using a local neighborhood, for example 7*7 neighborhood

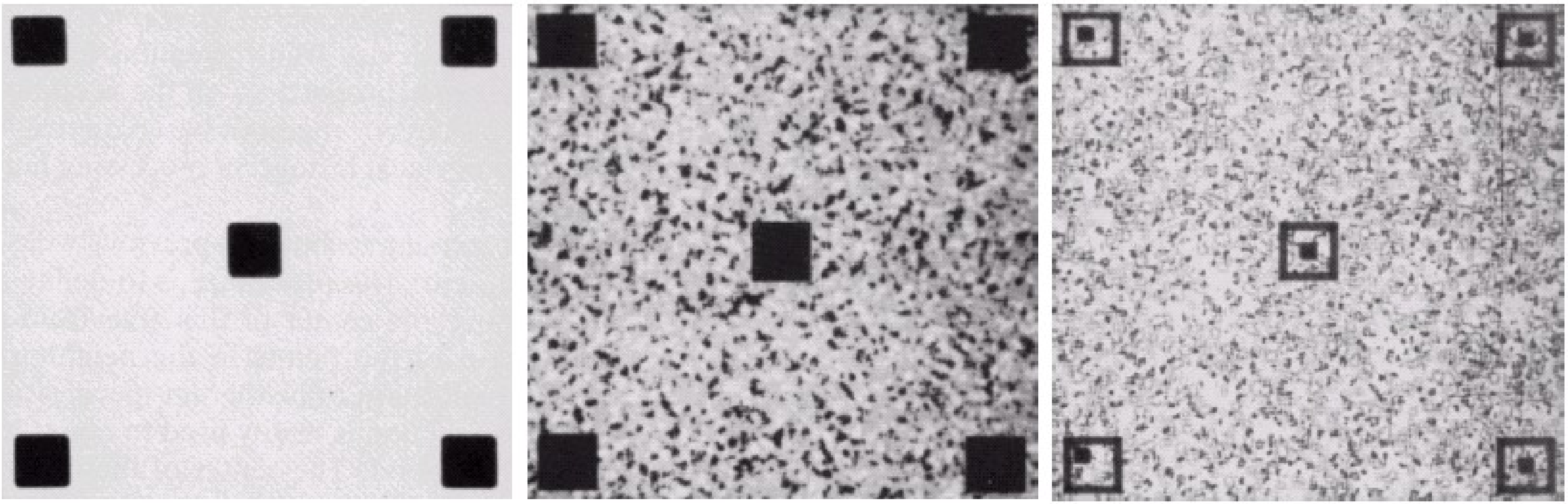

a b c

**FIGURE 3.23** (a) Original image. (b) Result of global histogram equalization. (c) Result of local histogram equalization using a $7 \times 7$ neighborhood about each pixel.

- Histogram using a local 3*3 neighborhood

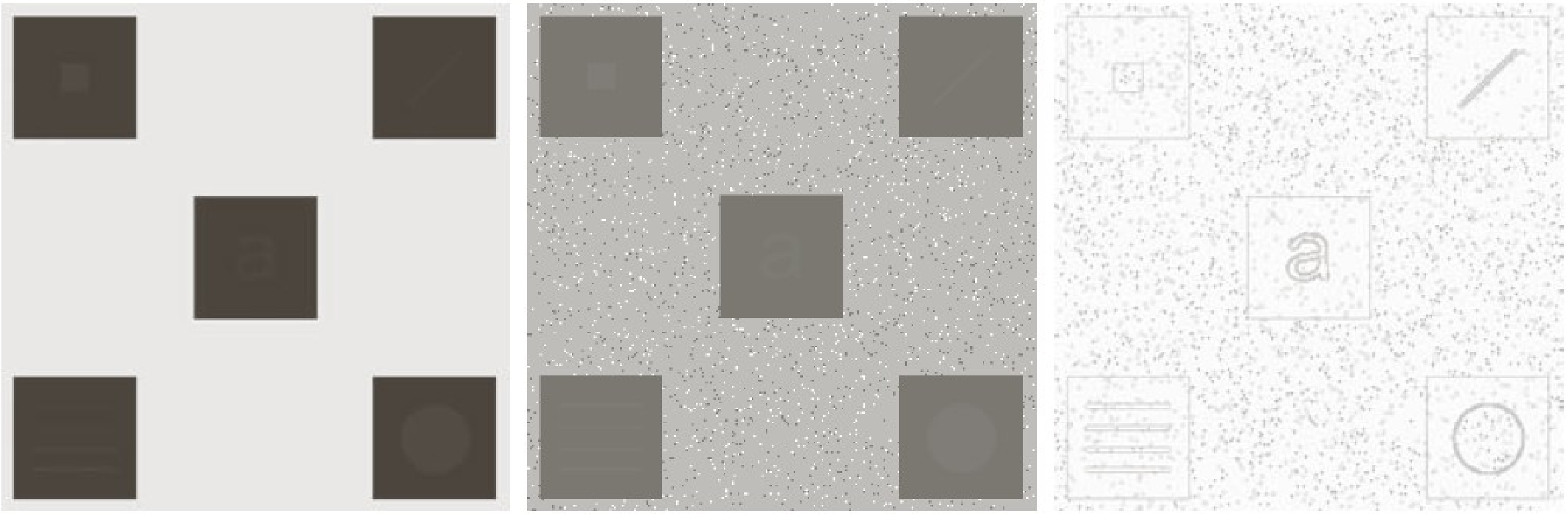

a b c

**FIGURE 3.26** (a) Original image. (b) Result of global histogram equalization. (c) Result of local histogram equalization applied to (a), using a neighborhood of size $3 \times 3$.

- Use of histogram statistics for image enhancement
  - $r$ denotes a discrete random variable
  - $p(r_i)$ denotes the normalized histogram component corresponding to the ith value of $r$
  - Mean

$$m = \sum_{i=0}^{L-1} r_i p(r_i)$$

- The nth moment

$$\mu_n(r) = \sum_{i=0}^{L-1} (r_i - m)^n p(r_i)$$

- The second moment

$$\mu_2(r) = \sum_{i=0}^{L-1} (r_i - m)^2 p(r_i)$$

- Global enhancement: The global mean and variance are measured over an entire image
- Local enhancement: The local mean and variance are used as the basis for making changes

- $r_{s,t}$ is the gray level at coordinates (s,t) in the neighborhood
- $p(r_{s,t})$ is the neighborhood normalized histogram component
- mean:

$$m_{S_{xy}} = \sum_{(s,t)\in S_{xy}} r_{s,t}\, p(r_{s,t})$$

- local variance

$$\sigma^2_{S_{xy}} = \sum_{(s,t)\in S_{xy}} [r_{s,t} - m_{S_{xy}}]^2\, p(r_{s,t})$$

- $E, k_0, k_1, k_2$ are specified parameters
- $M_G$ is the global mean
- $D_G$ is the global standard deviation
- Mapping

$$g(x,y) = \begin{cases} E \cdot f(x,y) & \text{if } m_{S_{xy}} \le k_0 M_G \text{ and } k_1 D_G \le \sigma_{S_{xy}} \le k_2 D_G \\ f(x,y) & \text{otherwise} \end{cases}$$

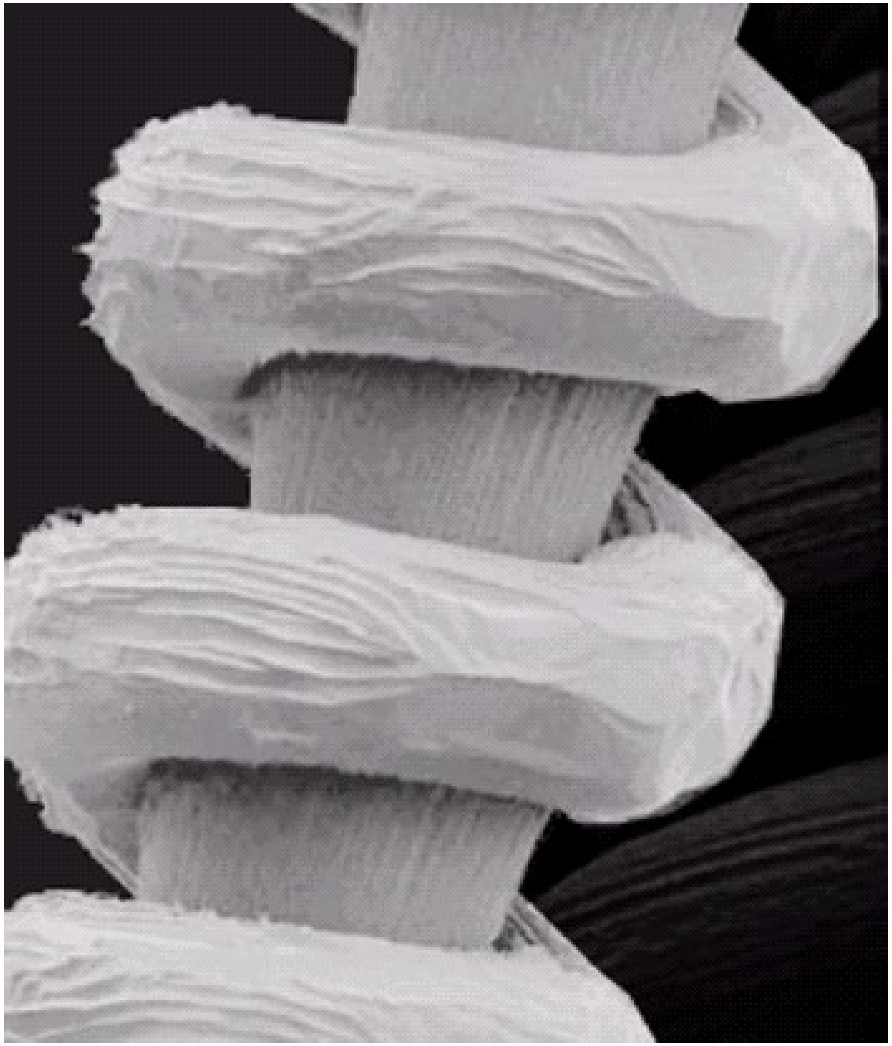

**FIGURE 3.24** SEM image of a tungsten filament and support, magnified approximately 130×. (Original image courtesy of Mr. Michael Shaffer, Department of Geological Sciences, University of Oregon, Eugene).

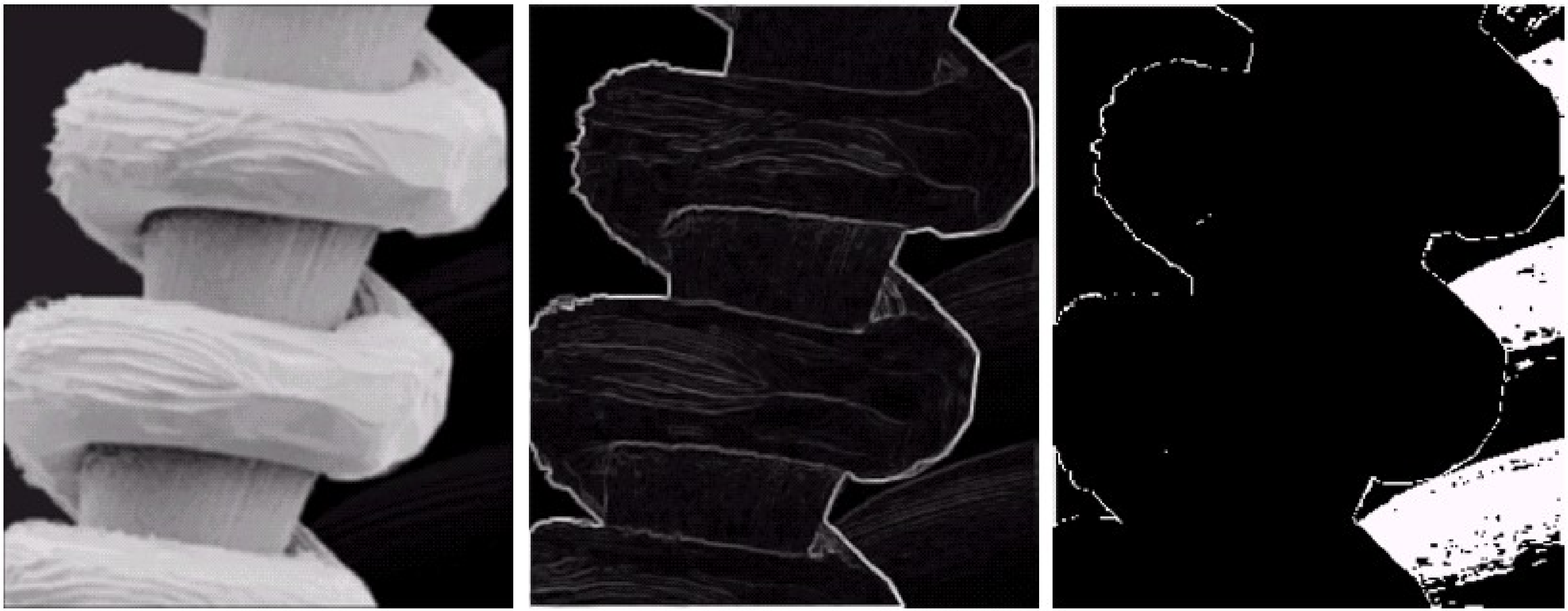

a b c

**FIGURE 3.25** (a) Image formed from all local means obtained from Fig. 3.24 using Eq. (3.3-21). (b) Image formed from all local standard deviations obtained from Fig. 3.24 using Eq. (3.3-22). (c) Image formed from all multiplication constants used to produce the enhanced image shown in Fig. 3.26.

**FIGURE 3.26** Enhanced SEM image. Compare with Fig. 3.24. Note in particular the enhanced area on the right side of the image.

# Fundamentals of Spatial Filtering

- The Mechanics of Spatial Filtering

$$
\begin{aligned}
R = {} & w(-1,-1) f(x-1, y-1) + \\
& w(-1,0) f(x-1, y) + \cdots + \\
& w(0,0) f(x, y) + \cdots + \\
& w(1,0) f(x+1, y) + \\
& w(1,1) f(x+1, y+1)
\end{aligned}
$$

- Image size: $M \times N$
- Mask size: $m \times n$

$$g(x,y) = \sum_{s=-a}^{a} \sum_{t=-b}^{b} w(s,t) f(x+s, y+t)$$

- $a = (m-1)/2$ and $b = (n-1)/2$
- $x = 0,1,2,\ldots,M-1$ and $y = 0,1,2,\ldots,N-1$

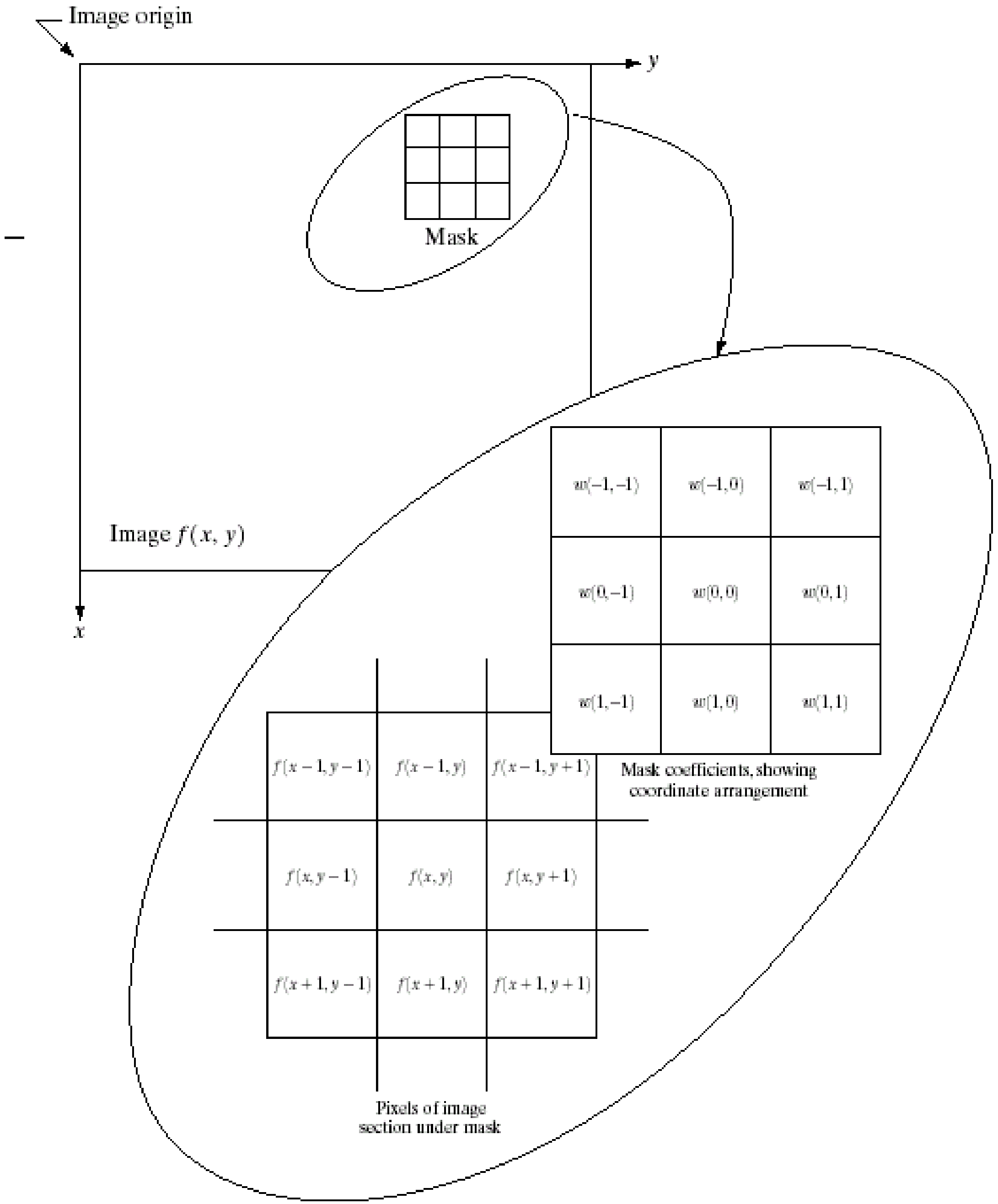


**FIGURE 3.32** The mechanics of spatial filtering. The magnified drawing shows a $3 \times 3$ mask and the image section directly under it; the image section is shown displaced out from under the mask for ease of readability.

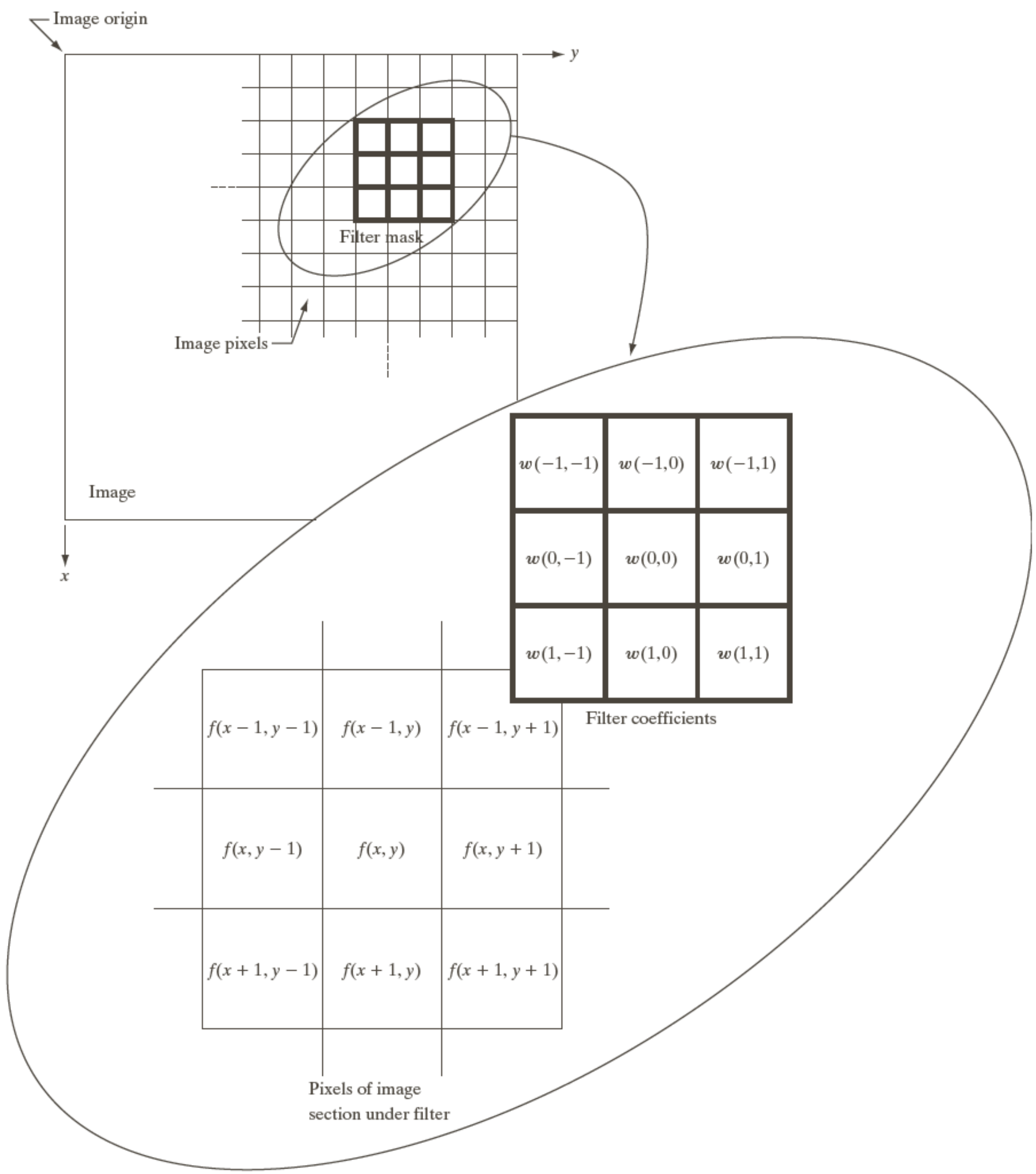


**FIGURE 3.28** The mechanics of linear spatial filtering using a 3 × 3 filter mask. The form chosen to denote the coordinates of the filter mask coefficients simplifies writing expressions for linear filtering.

# Spatial Correlation and Convolution

**Correlation**

| | Origin f | w |
|---|---|---|
| (a) | 0 0 0 1 0 0 0 0 | 1 2 3 2 8 |

(b)
```
        0 0 0 1 0 0 0 0
1 2 3 2 8
        Starting position alignment
```

(c)
```
Zero padding
0 0 0 0 0 0 0 1 0 0 0 0 0 0 0 0
1 2 3 2 8
```

(d)
```
0 0 0 0 0 0 0 1 0 0 0 0 0 0 0 0
  1 2 3 2 8
  Position after one shift
```

(e)
```
0 0 0 0 0 0 0 1 0 0 0 0 0 0 0 0
        1 2 3 2 8
        Position after four shifts
```

(f)
```
0 0 0 0 0 0 0 1 0 0 0 0 0 0 0 0
                      1 2 3 2 8
        Final position
```

Full correlation result

(g) 0 0 0 8 2 3 2 1 0 0 0 0

Cropped correlation result

(h) 0 8 2 3 2 1 0 0

**Convolution**

| Origin f | w rotated 180° | |
|---|---|---|
| 0 0 0 1 0 0 0 0 | 8 2 3 2 1 | (i) |

```
        0 0 0 1 0 0 0 0      (j)
8 2 3 2 1
```

```
0 0 0 0 0 0 0 1 0 0 0 0 0 0 0 0   (k)
8 2 3 2 1
```

```
0 0 0 0 0 0 0 1 0 0 0 0 0 0 0 0   (l)
  8 2 3 2 1
```

```
0 0 0 0 0 0 0 1 0 0 0 0 0 0 0 0   (m)
        8 2 3 2 1
```

```
0 0 0 0 0 0 0 1 0 0 0 0 0 0 0 0   (n)
                      8 2 3 2 1
```

Full convolution result

0 0 0 1 2 3 2 8 0 0 0 0 (o)

Cropped convolution result

0 1 2 3 2 8 0 0 (p)

**FIGURE 3.29** Illustration of 1-D correlation and convolution of a filter with a discrete unit impulse. Note that correlation and convolution are functions of *displacement*.

Origin $f(x, y)$

| | | | | |
|---|---|---|---|---|
| 0 | 0 | 0 | 0 | 0 |
| 0 | 0 | 0 | 0 | 0 |
| 0 | 0 | 1 | 0 | 0 |
| 0 | 0 | 0 | 0 | 0 |
| 0 | 0 | 0 | 0 | 0 |

$w(x, y)$

| | | |
|---|---|---|
| 1 | 2 | 3 |
| 4 | 5 | 6 |
| 7 | 8 | 9 |

(a)

Padded $f$

| | | | | | | | | |
|---|---|---|---|---|---|---|---|---|
| 0 | 0 | 0 | 0 | 0 | 0 | 0 | 0 | 0 |
| 0 | 0 | 0 | 0 | 0 | 0 | 0 | 0 | 0 |
| 0 | 0 | 0 | 0 | 0 | 0 | 0 | 0 | 0 |
| 0 | 0 | 0 | 0 | 0 | 0 | 0 | 0 | 0 |
| 0 | 0 | 0 | 0 | 1 | 0 | 0 | 0 | 0 |
| 0 | 0 | 0 | 0 | 0 | 0 | 0 | 0 | 0 |
| 0 | 0 | 0 | 0 | 0 | 0 | 0 | 0 | 0 |
| 0 | 0 | 0 | 0 | 0 | 0 | 0 | 0 | 0 |
| 0 | 0 | 0 | 0 | 0 | 0 | 0 | 0 | 0 |

(b)

Initial position for $w$

| | | | | | | | | |
|---|---|---|---|---|---|---|---|---|
| 1 | 2 | 3 | 0 | 0 | 0 | 0 | 0 | 0 |
| 4 | 5 | 6 | 0 | 0 | 0 | 0 | 0 | 0 |
| 7 | 8 | 9 | 0 | 0 | 0 | 0 | 0 | 0 |
| 0 | 0 | 0 | 0 | 0 | 0 | 0 | 0 | 0 |
| 0 | 0 | 0 | 0 | 1 | 0 | 0 | 0 | 0 |
| 0 | 0 | 0 | 0 | 0 | 0 | 0 | 0 | 0 |
| 0 | 0 | 0 | 0 | 0 | 0 | 0 | 0 | 0 |
| 0 | 0 | 0 | 0 | 0 | 0 | 0 | 0 | 0 |
| 0 | 0 | 0 | 0 | 0 | 0 | 0 | 0 | 0 |

(c)

Full correlation result

| | | | | | | | | |
|---|---|---|---|---|---|---|---|---|
| 0 | 0 | 0 | 0 | 0 | 0 | 0 | 0 | 0 |
| 0 | 0 | 0 | 0 | 0 | 0 | 0 | 0 | 0 |
| 0 | 0 | 0 | 0 | 0 | 0 | 0 | 0 | 0 |
| 0 | 0 | 0 | 9 | 8 | 7 | 0 | 0 | 0 |
| 0 | 0 | 0 | 6 | 5 | 4 | 0 | 0 | 0 |
| 0 | 0 | 0 | 3 | 2 | 1 | 0 | 0 | 0 |
| 0 | 0 | 0 | 0 | 0 | 0 | 0 | 0 | 0 |
| 0 | 0 | 0 | 0 | 0 | 0 | 0 | 0 | 0 |
| 0 | 0 | 0 | 0 | 0 | 0 | 0 | 0 | 0 |

(d)

Cropped correlation result

| | | | | |
|---|---|---|---|---|
| 0 | 0 | 0 | 0 | 0 |
| 0 | 9 | 8 | 7 | 0 |
| 0 | 6 | 5 | 4 | 0 |
| 0 | 3 | 2 | 1 | 0 |
| 0 | 0 | 0 | 0 | 0 |

(e)

Rotated $w$

| | | | | | | | | |
|---|---|---|---|---|---|---|---|---|
| 9 | 8 | 7 | 0 | 0 | 0 | 0 | 0 | 0 |
| 6 | 5 | 4 | 0 | 0 | 0 | 0 | 0 | 0 |
| 3 | 2 | 1 | 0 | 0 | 0 | 0 | 0 | 0 |
| 0 | 0 | 0 | 0 | 0 | 0 | 0 | 0 | 0 |
| 0 | 0 | 0 | 0 | 1 | 0 | 0 | 0 | 0 |
| 0 | 0 | 0 | 0 | 0 | 0 | 0 | 0 | 0 |
| 0 | 0 | 0 | 0 | 0 | 0 | 0 | 0 | 0 |
| 0 | 0 | 0 | 0 | 0 | 0 | 0 | 0 | 0 |
| 0 | 0 | 0 | 0 | 0 | 0 | 0 | 0 | 0 |

(f)

Full convolution result

| | | | | | | | | |
|---|---|---|---|---|---|---|---|---|
| 0 | 0 | 0 | 0 | 0 | 0 | 0 | 0 | 0 |
| 0 | 0 | 0 | 0 | 0 | 0 | 0 | 0 | 0 |
| 0 | 0 | 0 | 0 | 0 | 0 | 0 | 0 | 0 |
| 0 | 0 | 0 | 1 | 2 | 3 | 0 | 0 | 0 |
| 0 | 0 | 0 | 4 | 5 | 6 | 0 | 0 | 0 |
| 0 | 0 | 0 | 7 | 8 | 9 | 0 | 0 | 0 |
| 0 | 0 | 0 | 0 | 0 | 0 | 0 | 0 | 0 |
| 0 | 0 | 0 | 0 | 0 | 0 | 0 | 0 | 0 |
| 0 | 0 | 0 | 0 | 0 | 0 | 0 | 0 | 0 |

(g)

Cropped convolution result

| | | | | |
|---|---|---|---|---|
| 0 | 0 | 0 | 0 | 0 |
| 0 | 1 | 2 | 3 | 0 |
| 0 | 4 | 5 | 6 | 0 |
| 0 | 7 | 8 | 9 | 0 |
| 0 | 0 | 0 | 0 | 0 |

(h)

**FIGURE 3.30** Correlation (middle row) and convolution (last row) of a 2-D filter with a 2-D discrete, unit impulse. The 0s are shown in gray to simplify visual analysis.

- Vector Representation of Linear Filtering

$$R = w_1 z_1 + w_2 z_2 + \ldots + w_9 z_9$$

$$= \sum_{i=1}^{9} w_i z_i$$

**FIGURE 3.33** Another representation of a general 3 × 3 spatial filter mask.

| | | |
|---|---|---|
| $w_1$ | $w_2$ | $w_3$ |
| $w_4$ | $w_5$ | $w_6$ |
| $w_7$ | $w_8$ | $w_9$ |

# Smoothing Spatial Filters

- Smoothing Linear Filters
  - Noise reduction
  - Smoothing of false contours
  - Reduction of irrelevant detail

$$R = \frac{1}{9}\sum_{i=1}^{9} z_i$$

$$\frac{1}{9} \times \begin{array}{|c|c|c|} \hline 1 & 1 & 1 \\ \hline 1 & 1 & 1 \\ \hline 1 & 1 & 1 \\ \hline \end{array} \qquad \frac{1}{16} \times \begin{array}{|c|c|c|} \hline 1 & 2 & 1 \\ \hline 2 & 4 & 2 \\ \hline 1 & 2 & 1 \\ \hline \end{array}$$

$$g(x,y)=\frac{\sum_{s=-a}^{a}\sum_{t=-b}^{b} w(s,t)\,f(x+s,y+t)}{\sum_{s=-a}^{a}\sum_{t=-b}^{b} w(s,t)}$$

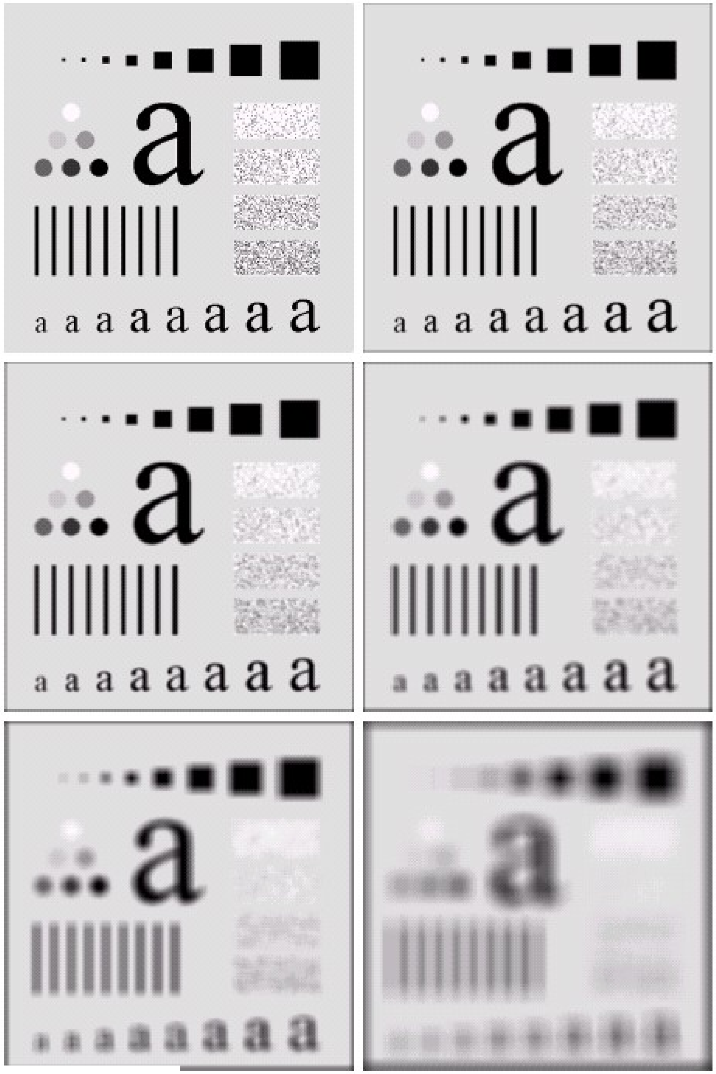

a b
c d
e f

**FIGURE 3.35** (a) Original image, of size 500 × 500 pixels. (b)–(f) Results of smoothing with square averaging filter masks of sizes $n = 3, 5, 9, 15$, and 35, respectively. The black squares at the top are of sizes 3, 5, 9, 15, 25, 35, 45, and 55 pixels, respectively; their borders are 25 pixels apart. The letters at the bottom range in size from 10 to 24 points, in increments of 2 points; the large letter at the top is 60 points. The vertical bars are 5 pixels wide and 100 pixels high; their separation is 20 pixels. The diameter of the circles is 25 pixels, and their borders are 15 pixels apart; their gray levels range from 0% to 100% black in increments of 20%. The background of the image is 10% black. The noisy rectangles are of size 50 × 120 pixels.

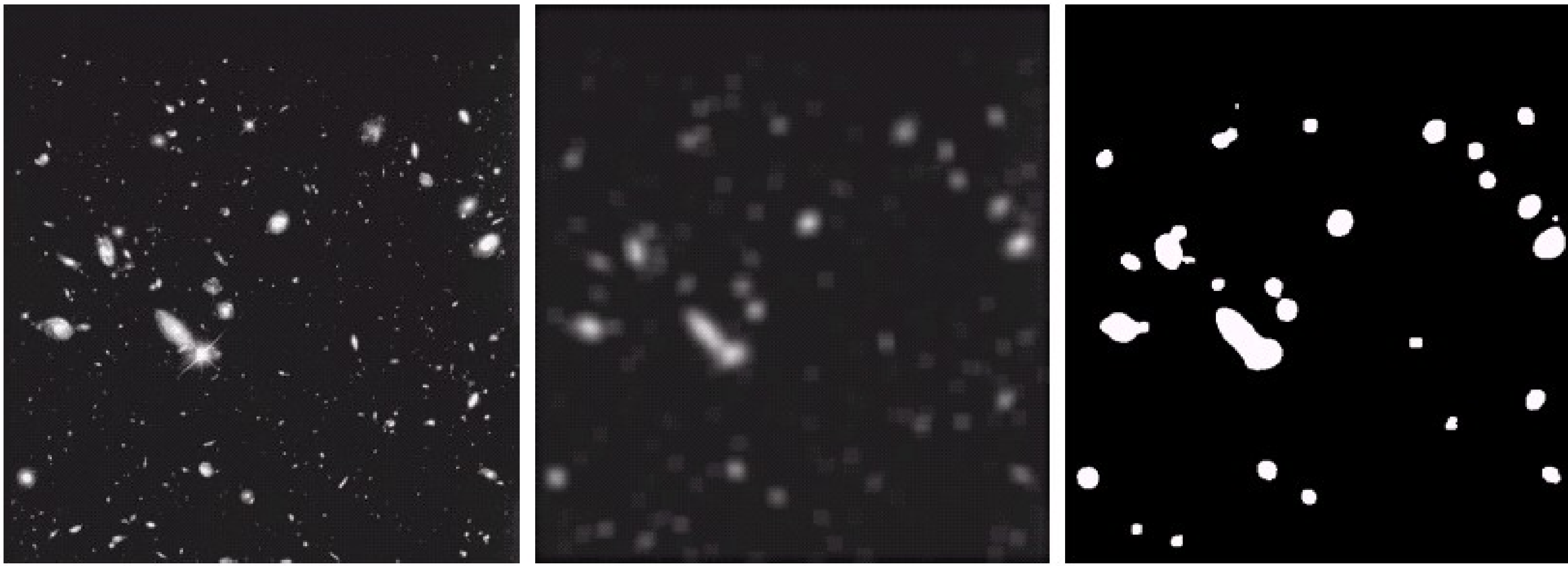

a b c

**FIGURE 3.36** (a) Image from the Hubble Space Telescope. (b) Image processed by a 15 × 15 averaging mask. (c) Result of thresholding (b). (Original image courtesy of NASA.)

- Order-statistic filters
  - median filter: Replace the value of a pixel by the median of the gray levels in the neighborhood of that pixel
  - Noise-reduction

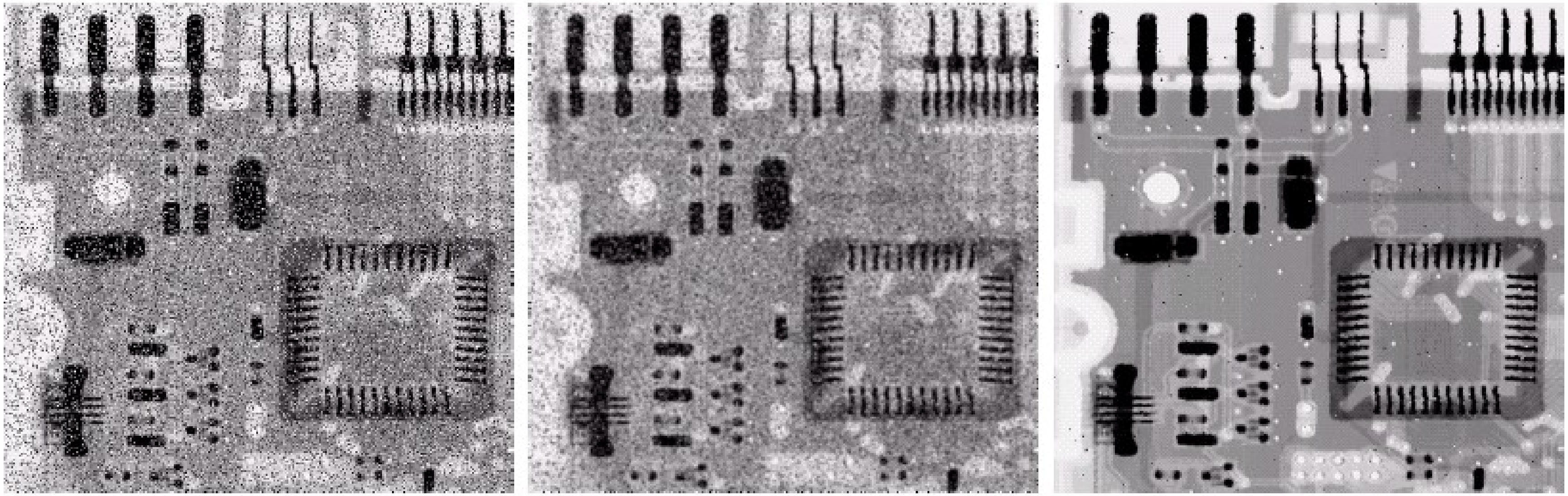

a b c

**FIGURE 3.37** (a) X-ray image of circuit board corrupted by salt-and-pepper noise. (b) Noise reduction with a $3 \times 3$ averaging mask. (c) Noise reduction with a $3 \times 3$ median filter. (Original image courtesy of Mr. Joseph E. Pascente, Lixi, Inc.)

# Sharpening Spatial Filters

- Foundation
  - The first-order derivative

$$\frac{\partial f}{\partial x} = f(x+1) - f(x)$$

  - The second-order derivative

$$\frac{\partial^2 f}{\partial x^2} = f(x+1) + f(x-1) - 2f(x)$$

a b
c

**FIGURE 3.38** (a) A simple image. (b) 1-D horizontal gray-level profile along the center of the image and including the isolated noise point. (c) Simplified profile (the points are joined by dashed lines to simplify interpretation).

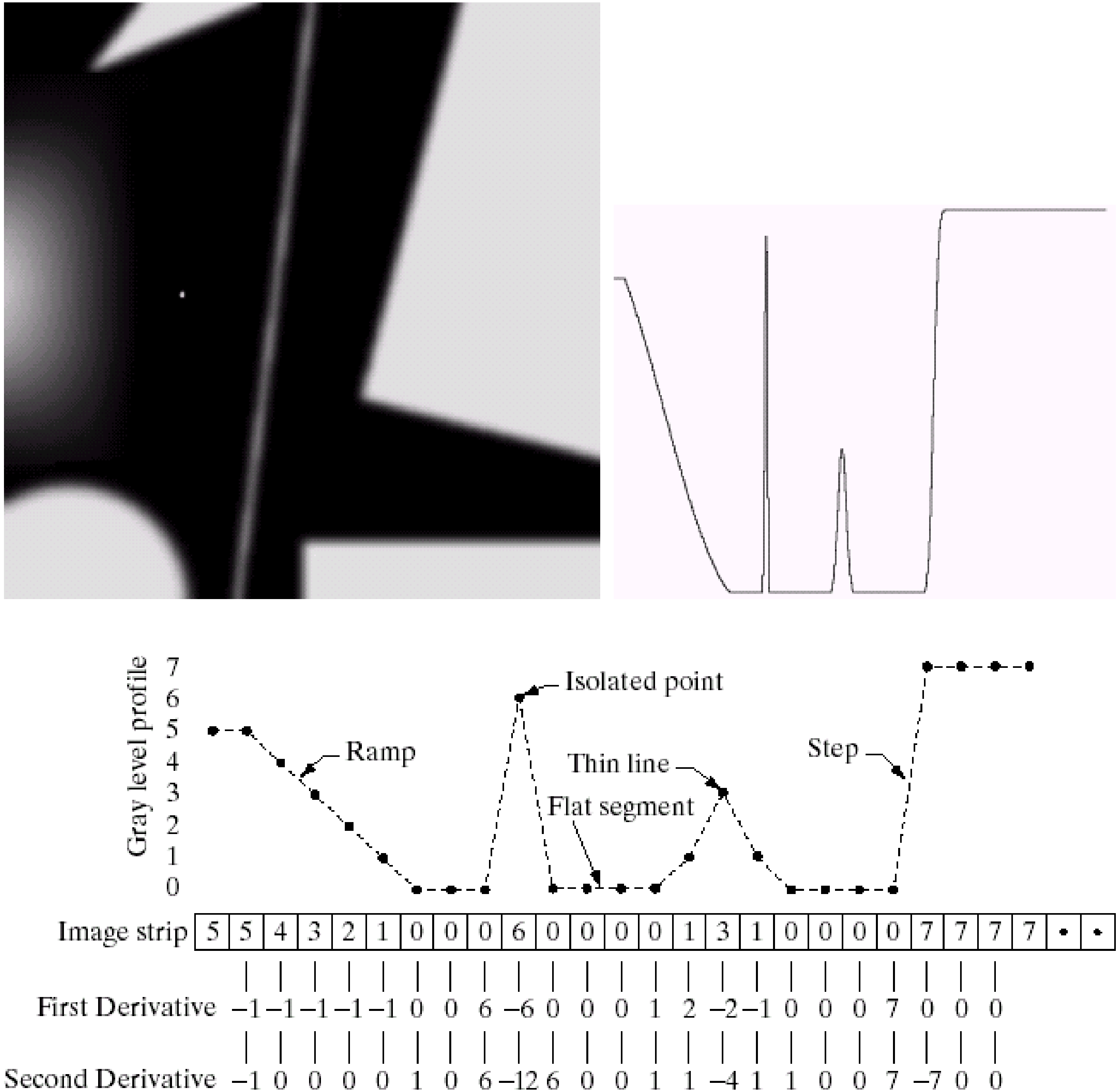

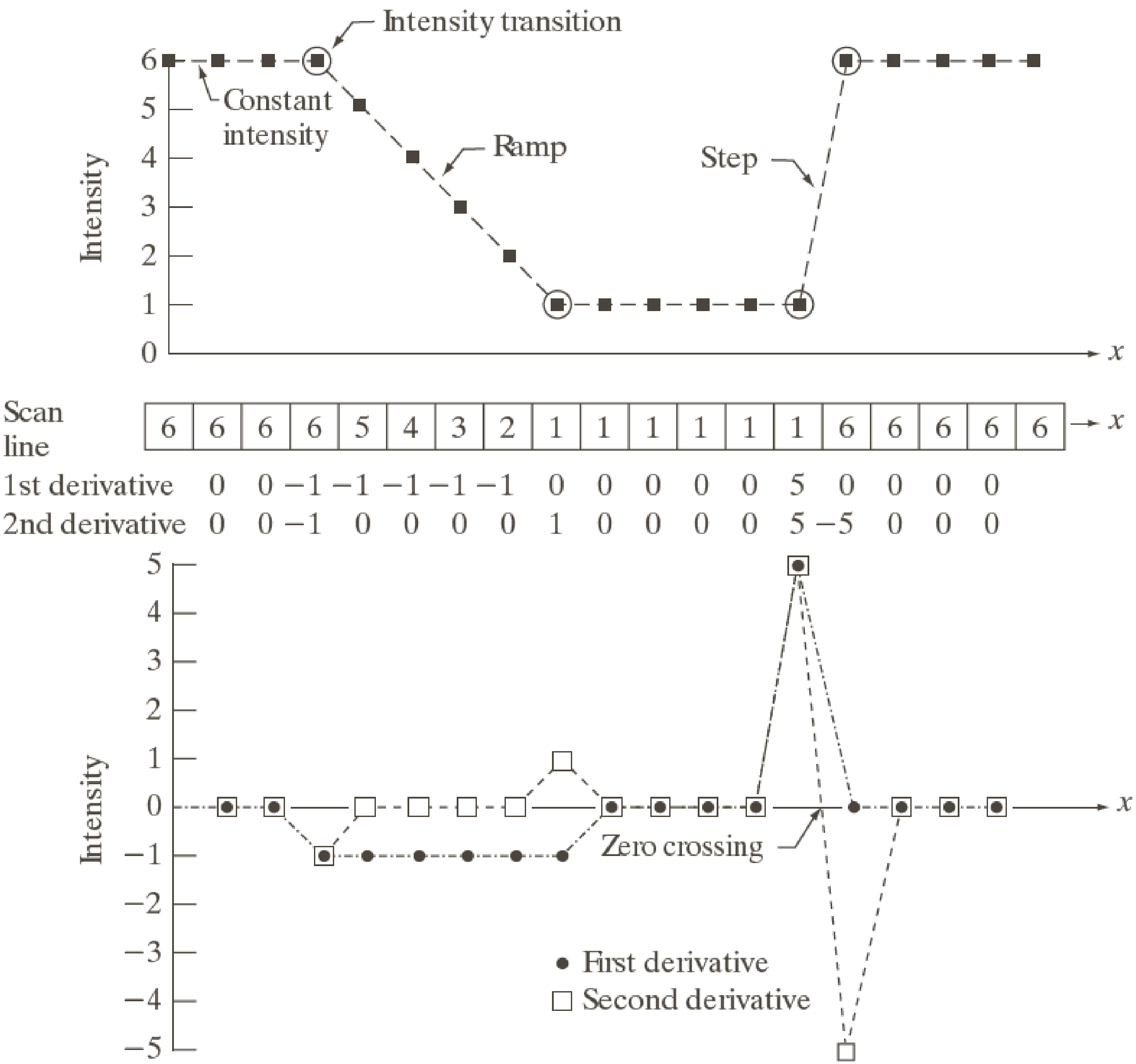


a
b
c

**FIGURE 3.36** Illustration of the first and second derivatives of a 1-D digital function representing a section of a horizontal intensity profile from an image. In (a) and (c) data points are joined by dashed lines as a visualization aid.

- Use of second derivatives for enhancement-The Laplacian
  - Development of the method

$$\nabla^2 f = \frac{\partial^2 f}{\partial x^2} + \frac{\partial^2 f}{\partial y^2}$$

$$\frac{\partial^2 f}{\partial x^2} = f(x+1, y) + f(x-1, y) - 2f(x, y)$$

$$\frac{\partial^2 f}{\partial y^2} = f(x, y+1) + f(x, y-1) - 2f(x, y)$$

$$\nabla^2 f = [f(x+1, y) + f(x-1, y) + f(x, y+1) + f(x, y-1)] - 4f(x, y)$$

$$g(x,y) = \begin{cases} f(x,y) - \nabla^2 f(x,y) & \text{if the center coefficient of the Laplacian mask is negative} \\ f(x,y) + \nabla^2 f(x,y) & \text{if the center coefficient of the Laplacian mask is positive} \end{cases}$$

| | | |
|---|---|---|
| 0 | 1 | 0 |
| 1 | −4 | 1 |
| 0 | 1 | 0 |

| | | |
|---|---|---|
| 1 | 1 | 1 |
| 1 | −8 | 1 |
| 1 | 1 | 1 |

| | | |
|---|---|---|
| 0 | −1 | 0 |
| −1 | 4 | −1 |
| 0 | −1 | 0 |

| | | |
|---|---|---|
| −1 | −1 | −1 |
| −1 | 8 | −1 |
| −1 | −1 | −1 |

| | |
|---|---|
| a | b |
| c | d |

**FIGURE 3.39**
(a) Filter mask used to implement the digital Laplacian, as defined in Eq. (3.7-4). (b) Mask used to implement an extension of this equation that includes the diagonal neighbors. (c) and (d) Two other implementations of the Laplacian.

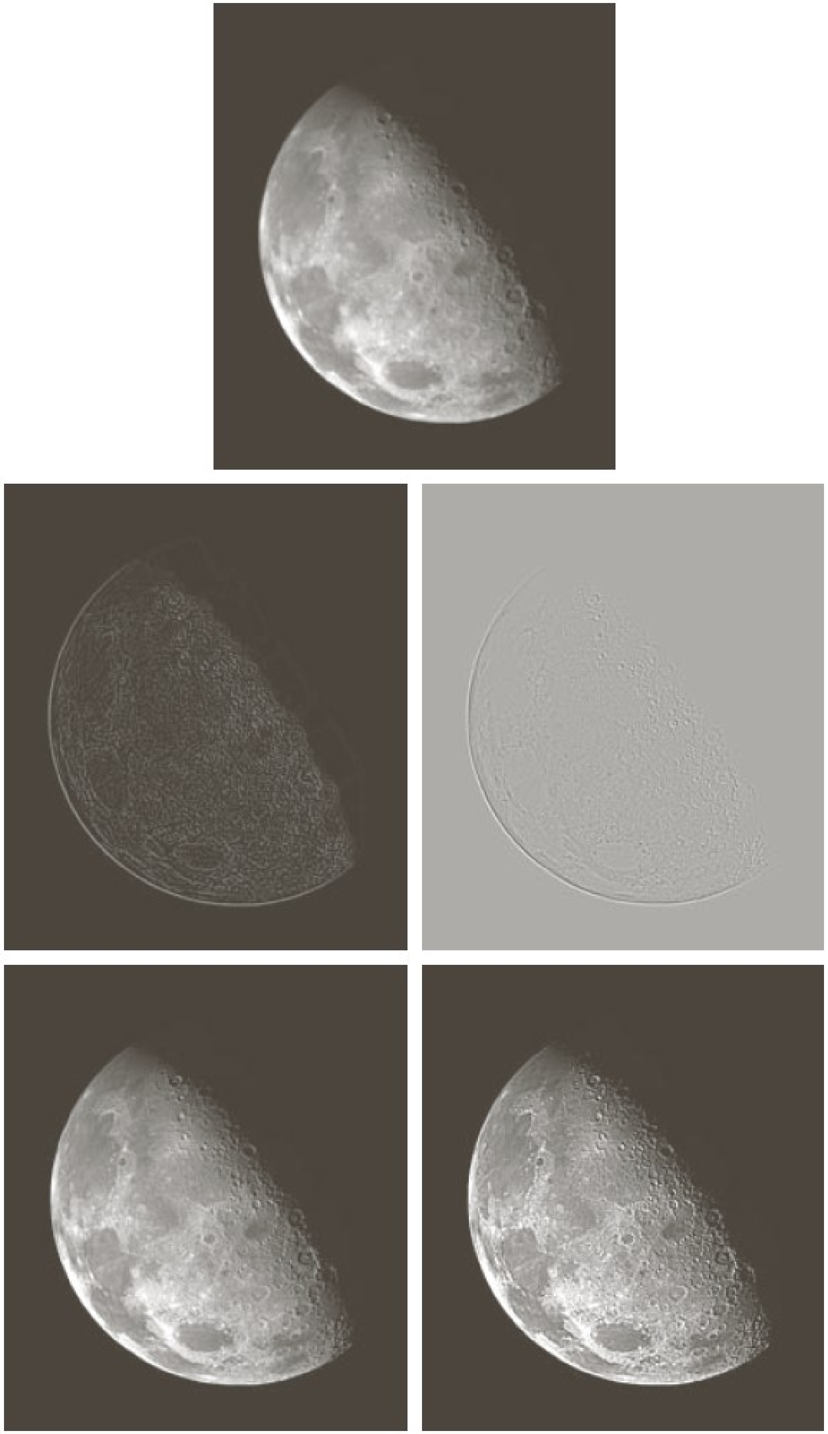

| | | |
|---|---|---|
| | a | |
| b | c | |
| d | e | |

**FIGURE 3.38**
(a) Blurred image of the North Pole of the moon. (b) Laplacian without scaling. (c) Laplacian with scaling. (d) Image sharpened using the mask in Fig. 3.37(a). (e) Result of using the mask in Fig. 3.37(b). (Original image courtesy of NASA.)

- Simplifications

$$g(x,y) = f(x,y) - [f(x+1,y) + f(x-1,y) + f(x,y+1) +$$
$$f(x,y-1)] + 4f(x,y)$$
$$= 5f(x,y) - [f(x+1,y) + f(x-1,y) + f(x,y+1) +$$
$$f(x,y-1)]$$

| | | |
|---|---|---|
| 0 | −1 | 0 |
| −1 | 5 | −1 |
| 0 | −1 | 0 |

| | | |
|---|---|---|
| −1 | −1 | −1 |
| −1 | 9 | −1 |
| −1 | −1 | −1 |

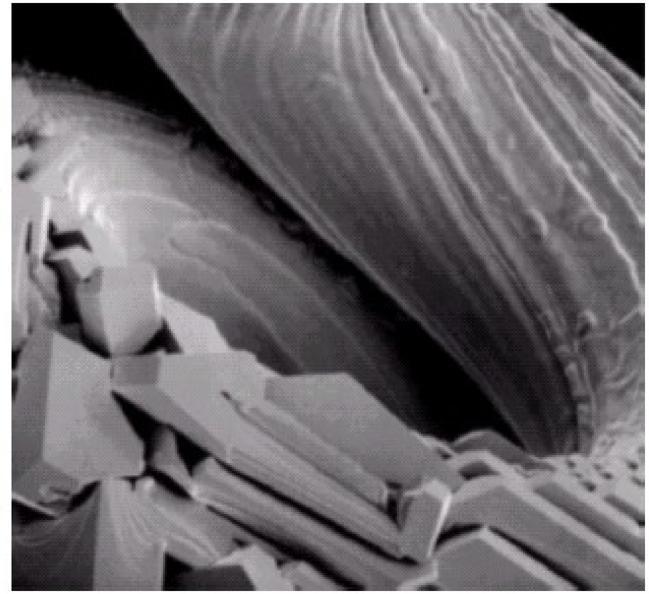

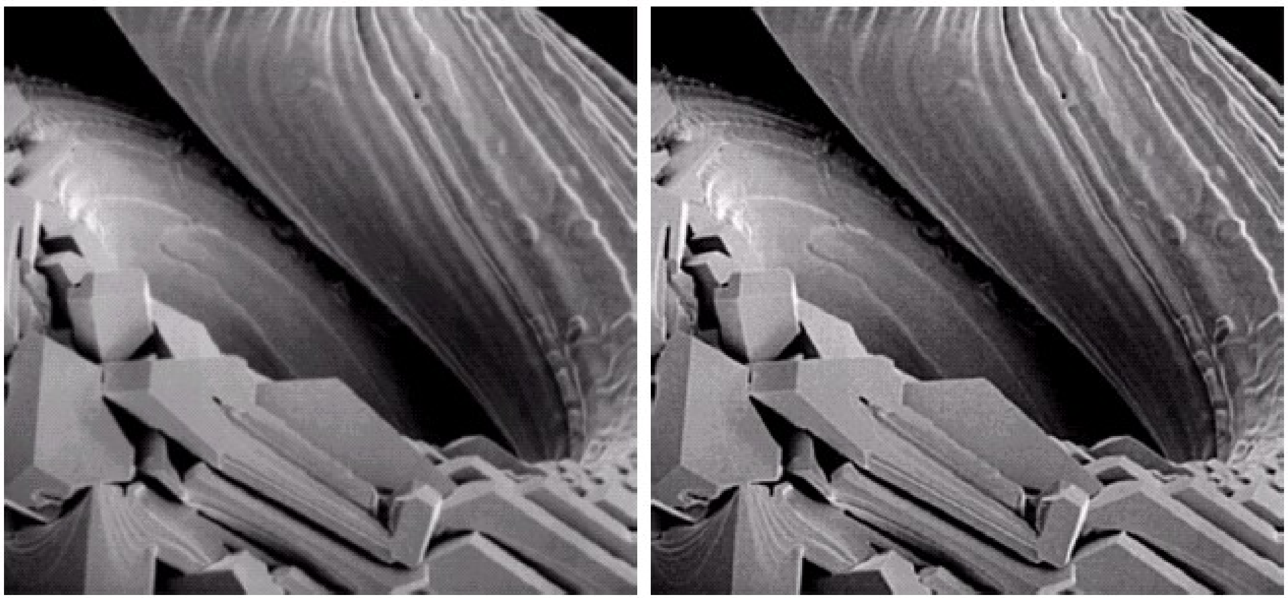

a b c
d e

**FIGURE 3.41** (a) Composite Laplacian mask. (b) A second composite mask. (c) Scanning electron microscope image. (d) and (e) Results of filtering with the masks in (a) and (b), respectively. Note how much sharper (e) is than (d). (Original image courtesy of Mr. Michael Shaffer, Department of Geological Sciences, University of Oregon, Eugene.)

- Unsharp masking and highboost filtering
  - Unsharp masking
    - Substract a blurred version of an image from the image itself

$$g_{mask}(x,y) = f(x,y) - \bar{f}(x,y)$$

- $f(x,y)$: The image, $\bar{f}(x,y)$ : The blurred image

$$g(x,y) = f(x,y) + k * g_{mask}(x,y) \qquad ,k = 1$$

- High-boost filtering

$$g(x, y) = f(x, y) + k * g_{mask}(x, y) \qquad , k > 1$$

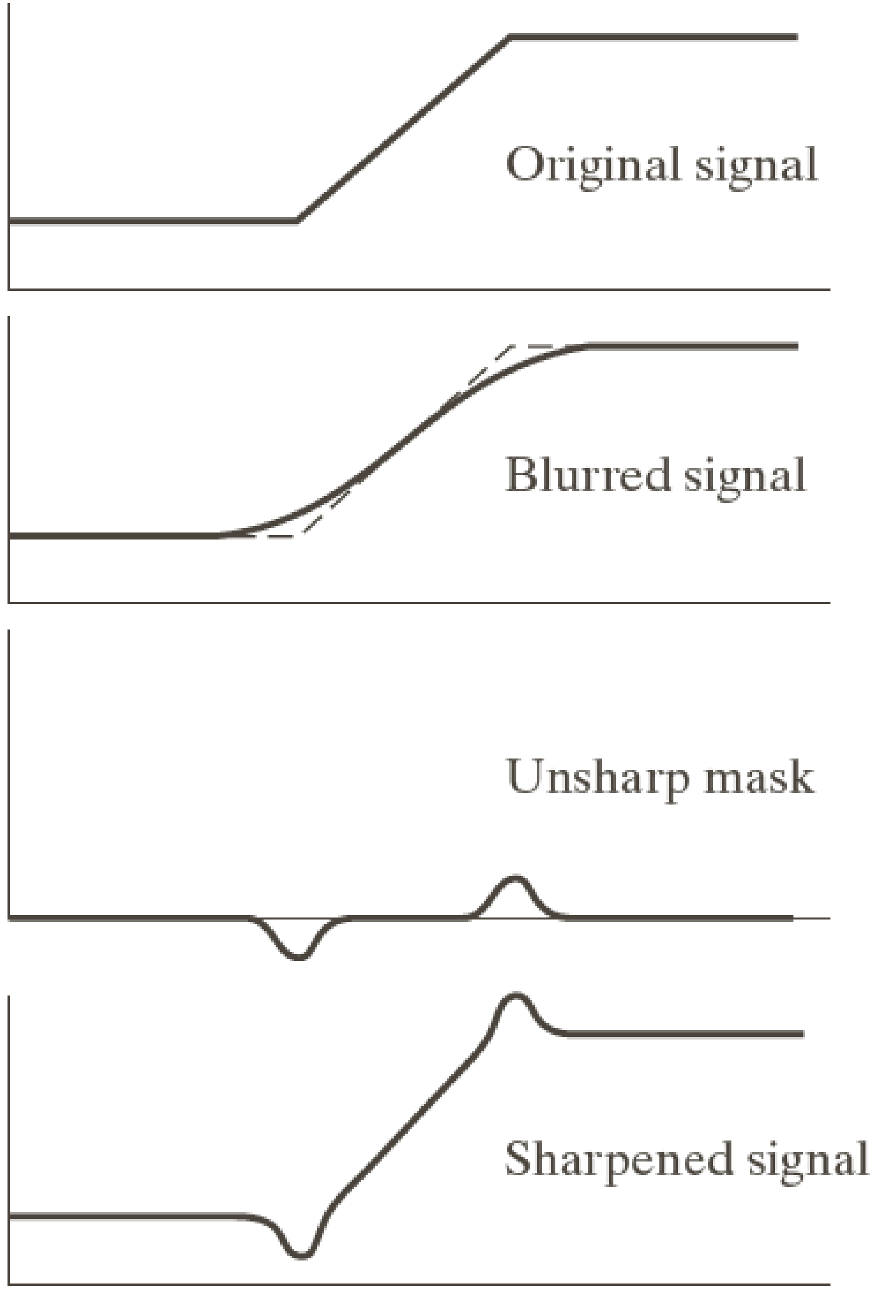


a
b
c
d

**FIGURE 3.39** 1-D illustration of the mechanics of unsharp masking. (a) Original signal. (b) Blurred signal with original shown dashed for reference. (c) Unsharp mask. (d) Sharpened signal, obtained by adding (c) to (a).


a
b
c
d
e

**FIGURE 3.40**
(a) Original image.
(b) Result of blurring with a Gaussian filter.
(c) Unsharp mask. (d) Result of using unsharp masking.
(e) Result of using highboost filtering.

- Using first-order derivatives for (nonlinear) image sharpening—The gradient

$$\nabla \mathbf{f} = \begin{bmatrix} G_x \\ G_y \end{bmatrix} = \begin{bmatrix} \dfrac{\partial f}{\partial x} \\ \dfrac{\partial f}{\partial y} \end{bmatrix}$$

- The magnitude is rotation invariant (isotropic)

$$\nabla f = \mathrm{mag}(\nabla \mathbf{f}) = \left[G_x^2 + G_y^2\right]^{1/2}$$

$$= \left[\left(\frac{\partial f}{\partial x}\right)^2 + \left(\frac{\partial f}{\partial y}\right)^2\right]^{1/2}$$

$$\nabla f \approx \left|G_x\right| + \left|G_y\right|$$

- Computing using cross differences, Roberts cross-gradient operators

$$G_x = (z_9 - z_5) \quad \text{and} \quad G_y = (z_8 - z_6)$$

$$\nabla f = \left[ (z_9 - z_5)^2 + (z_8 - z_6)^2 \right]^{1/2}$$

$$\nabla f \approx |z_9 - z_5| + |z_8 - z_6|$$

- Sobel operators
  - A weight value of 2 is to achieve some smoothing by giving more importance to the center point

$$\nabla f \approx \left|(z_7 + 2z_8 + z_9) - (z_1 + 2z_2 + z_3)\right| + \left|(z_3 + 2z_6 + z_9) - (z_1 + 2z_4 + z_7)\right|$$

a
b c
d e

**FIGURE 3.44** A 3 × 3 region of an image (the $z$'s are gray-level values) and masks used to compute the gradient at point labeled $z_5$. All masks coefficients sum to zero, as expected of a derivative operator.

| | | |
|---|---|---|
| $z_1$ | $z_2$ | $z_3$ |
| $z_4$ | $z_5$ | $z_6$ |
| $z_7$ | $z_8$ | $z_9$ |

| | |
|---|---|
| −1 | 0 |
| 0 | 1 |

| | |
|---|---|
| 0 | −1 |
| 1 | 0 |

| | | |
|---|---|---|
| −1 | −2 | −1 |
| 0 | 0 | 0 |
| 1 | 2 | 1 |

| | | |
|---|---|---|
| −1 | 0 | 1 |
| −2 | 0 | 2 |
| −1 | 0 | 1 |

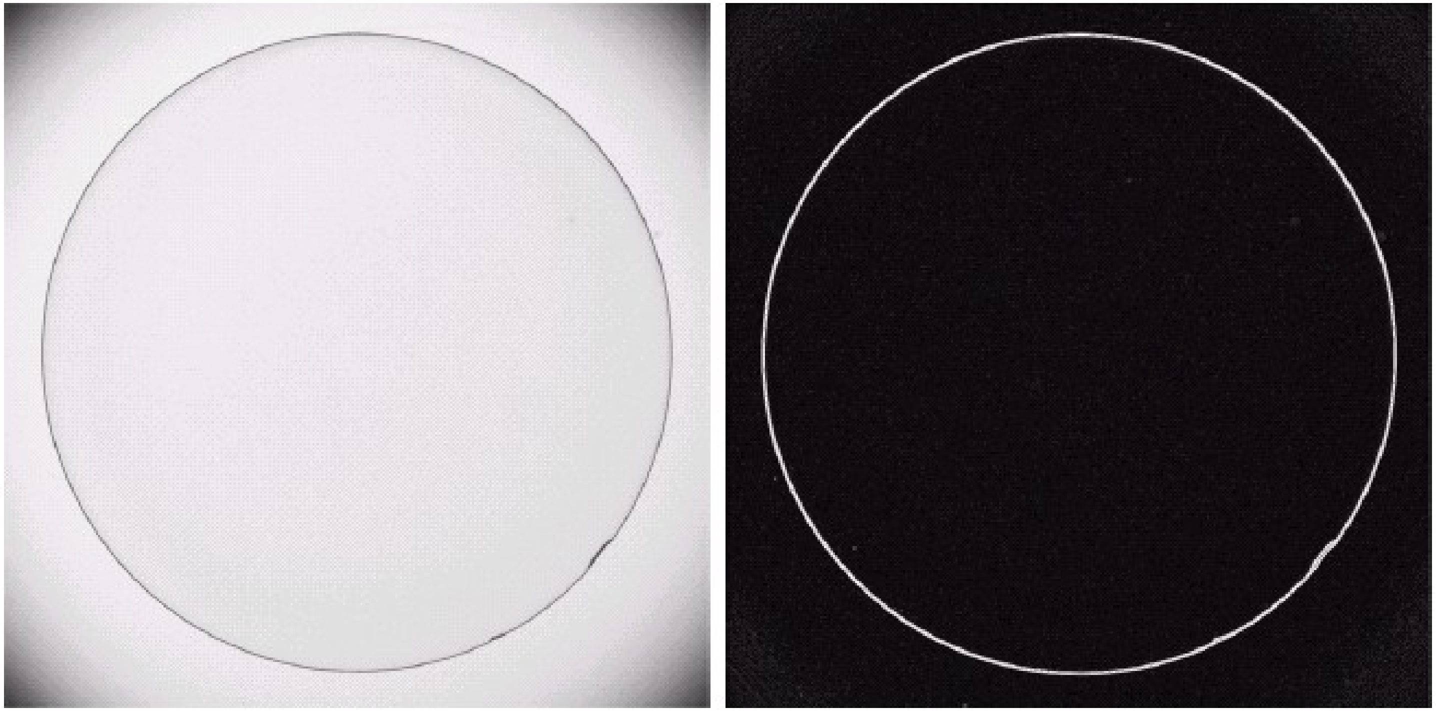

a b

**FIGURE 3.45** Optical image of contact lens (note defects on the boundary at 4 and 5 o'clock). (b) Sobel gradient. (Original image courtesy of Mr. Pete Sites, Perceptics Corporation.)

# Combining Spatial Enhancement Methods

- An example
  - Laplacian to highlight fine detail
  - Gradient to enhance prominent edges
  - Smoothed version of the gradient image used to mask the Laplacian image
  - Increase the dynamic range of the gray levels by using a gray-level transformation

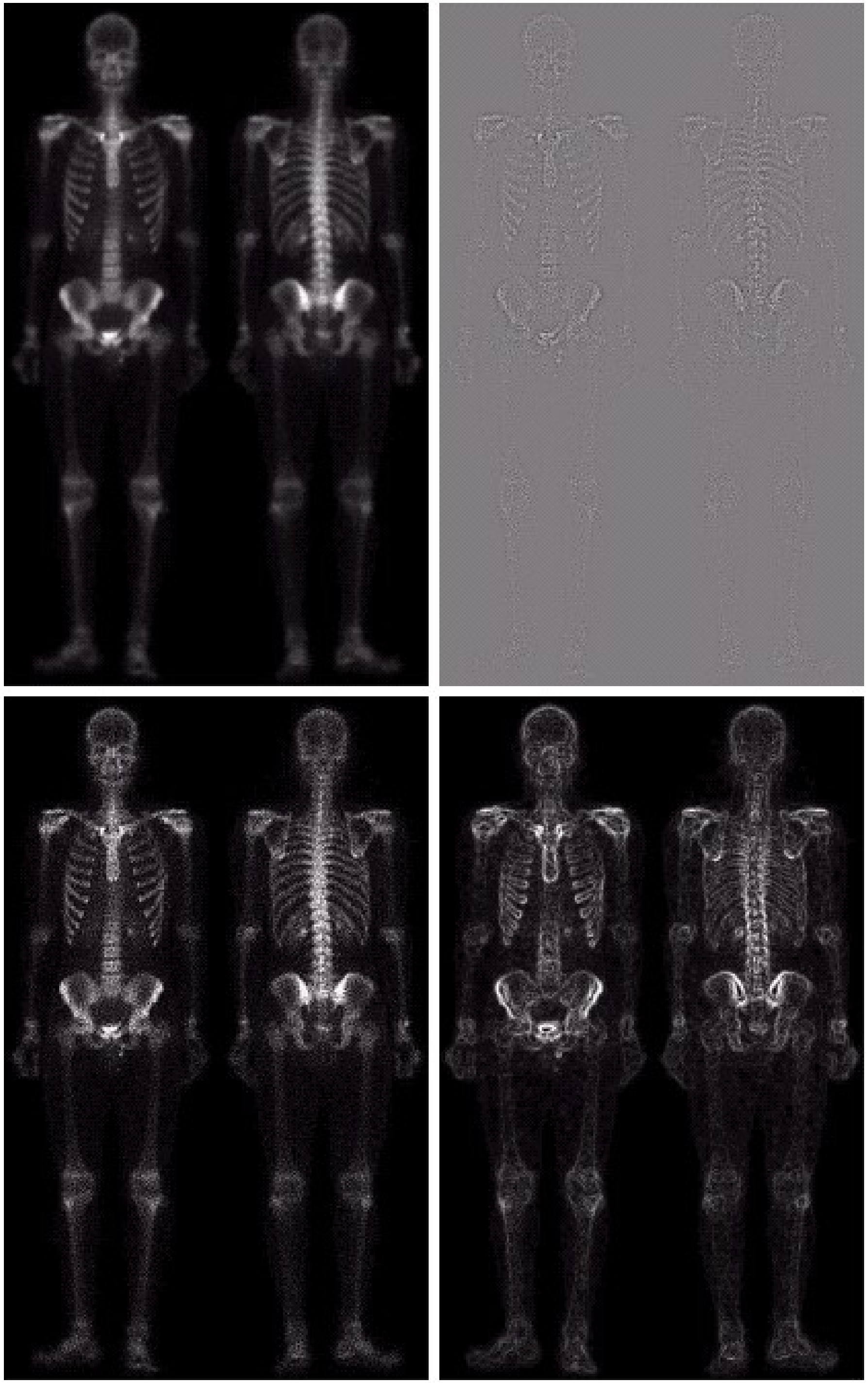

| a | b |
|---|---|
| c | d |

**FIGURE 3.46** (a) Image of whole body bone scan. (b) Laplacian of (a). (c) Sharpened image obtained by adding (a) and (b). (d) Sobel of (a).

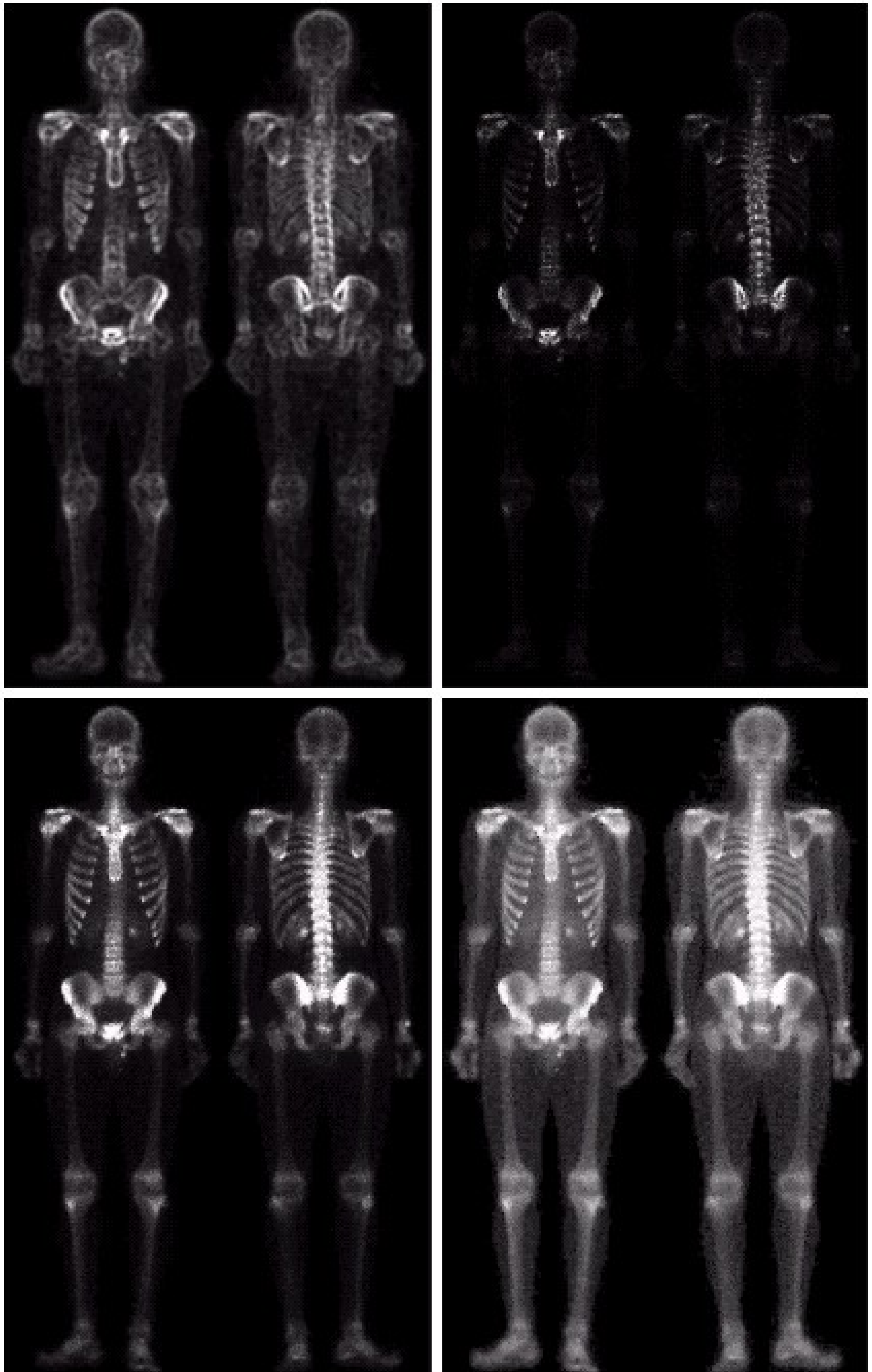

| e | f |
|---|---|
| g | h |

**FIGURE 3.46** *(Continued)* (e) Sobel image smoothed with a $5 \times 5$ averaging filter. (f) Mask image formed by the product of (c) and (e). (g) Sharpened image obtained by the sum of (a) and (f). (h) Final result obtained by applying a power-law transformation to (g). Compare (g) and (h) with (a). (Original image courtesy of G.E. Medical Systems.)